Seismic performance of composite plate shear walls

Sandip Dey, Anjan K. Bhowmick

PII: S2352-0124(16)00015-1
DOI: doi: 10.1016/j.istruc.2016.01.006
Reference: ISTRUC 88

To appear in:

Received date: 10 February 2015
Revised date: 21 December 2015
Accepted date: 25 January 2016

Please cite this article as: Dey Sandip, Bhowmick Anjan K., Seismic performance of composite plate shear walls, (2016), doi: 10.1016/j.istruc.2016.01.006

Seismic performance of composite plate shear walls

Sandip Dey and Anjan K Bhowmick

Department of Building, Civil and Environmental Engineering, Concordia University, Montreal, Quebec, Canada

Abstract: Nonlinear seismic responses of a 4-storey and 6-storey composite plate shear wall (C-PSW) are studied. A nonlinear finite element model which includes both material and geometric nonlinearities is used for this study. Nonlinear seismic analysis shows that composite plate shear walls, in high seismic region, behave in a stable and ductile manner. It has been observed that the boundary members and the reinforced concrete panel of C-PSW carry significant amount of shear which is not considered in design of C-PSW in AISC 341-10. The study also shows that design axial forces and moments in the boundary columns designed according to capacity design concepts are in good agreement with those of the nonlinear seismic analyses. A series of C-PSWs with different geometry are designed and analysed to evaluate the current period formula in building codes. It is observed that the current code predicts periods that are generally shorter than the periods obtained from finite element analysis. An improved simple formula for estimating the fundamental period of C-PSW is developed by regression analysis of the period data obtained from analysis of the selected C-PSWs. Finally, two equations for determining shear stud spacing and thickness of reinforced concrete panel for the C-PSWs are proposed.

Keywords: Composite Plate Shear Wall; Seismic Analysis; Fundamental Period; Shear Stud Spacing

1. Introduction

Shear walls have been long used as lateral load resisting systems. Some of the most commonly used shear walls in multistoried buildings are reinforced concrete (RC) shear walls and steel plate shear walls (SPSWs). In thin unstiffened SPSWs, infill plates tend to buckle with a very small applied lateral load. At the point of buckling, the load-resisting mechanism changes from in-plane shear to an inclined tension field. The tension field action developed in the infill plates is capable of resisting additional shear until they reach the yield strength. Thus, design and analysis of unstiffened SPSWs are based on the post-buckling strength of the infill panels. A significant research work, both experimental [1-7] and analytical [8-13], has been conducted on unstiffened SPSWs and it was shown that SPSWs are very effective system for resisting lateral loads due to wind and earthquakes. However, there are some disadvantages regarding the overall buckling of the steel plates that can cause the reduction in the shear strength, stiffness, and energy dissipation capacity [14]. Because of negligible out of plane stiffness SPSWs are not efficient in resisting accidental loads, such as blast and impact loading [13]. Also, steel is weak against fires and thus, like other steel lateral load resisting systems, SPSW must be protected against fire [13]. Moreover, in steel shear walls, due to large inelastic deformations of the steel plate, the connections of the boundary columns and beams can undergo large cyclic rotations and interstorey drifts [15]. On the other hand, concrete shear walls have their own disadvantages. During large cyclic displacements, they can develop tension cracks and localized crushing. Composite plate shear walls (C-PSWs) that consist of SPSWs connected with reinforced concrete panels on one or both sides of

the steel infill plates with bolts at regular intervals are expected to combine the advantages of steel and concrete shear walls. The layer of pre-cast or cast-in-situ reinforced concrete panel contributes to safeguard against fire, explosions etc.

To date very limited research has been done on C-PSWs. Research on composite plate shear wall started with Zhao and Astaneh-Asl [14]. They tested two three-story composite shear wall specimens under quasi-static cyclic loading, which they named innovative and traditional C-PSWs. The traditional C-PSW system had no gap between the concrete panel periphery and the surrounding steel boundary members. The innovative system on the other hand, had a 32 mm gap in between the concrete periphery and the boundary steel members. For both test specimens, the steel plates were bolted with reinforced concrete panels at regular intervals. It was reported that both specimens showed highly ductile behavior and stable cyclic post yielding performance. However, in the innovative system, damage to the concrete wall under relatively large cycles was less in comparison to a traditional system. Their study finally resulted in some design guidelines for C-PSW design, which have been adopted in AISC 341-10 [16]. Recent experimental studies on C-PSWs by Guo et al. [17, 18] also showed that C-PSW possessed good ductility and excellent energy dissipation capacity and in C-PSW system, the RC panels attached to steel plates were able to prevent the overall buckling of steel plate before yielding in shear and thus improved shear capacity. Though majority of the shear is resisted by the steel infill plate, similar to SPSW [10], it is expected that the boundary framing members will resist a significant portion of storey shear. In addition, the attached concrete panel is expected to resist a certain portion of storey shear. Current design guidelines for C-PSW

in AISC 341-10 do not have any requirements for the design of framing members so that they can resist a certain portion of the storey shear.

Experimental and analytical research on C-PSWs has focused mainly on static and quasi-static cyclic loading conditions. To date C-PSWs have not been studied under seismic loadings.

The objective of this research is to investigate the inelastic dynamic response of C-PSWs when subjected to severe ground motions, and thereby evaluate the degree to which the design procedures achieve the desired behavior. This paper presents the results, such as shear distribution between steel plate, columns and the concrete panel, design forces of boundary columns and interstorey drifts, of non-linear dynamic analyses of a typical 4-storey and a 6-storey C-PSW designed according to capacity design provisions, when subjected to compatible earthquake ground motions of Vancouver, Canada.

Shear studs which are used to connect the steel infill plate with the concrete panel should be properly spaced to ensure optimum performance of the composite plate shear wall. Recently, Rahai and Hatami [19] performed analytical and experimental studies on one-story C-PSWs with different geometries mainly to find out the effect of the distance between the shear studs on the overall behavior of the C-PSWs. Their experimental program consisted of three types of specimens: a single steel shear wall, three steel reinforced concrete composite walls and one steel flexible frame. The specimens were designed to undergo ductile modes of failure. Results from their analytical study indicated that with an increase in distance between the shear studs, the amount of energy

absorbed increases and thus improves ductility up to specific stud spacing, beyond which there is no difference. However, their study did not provide any guidelines on what would be the minimum or maximum spacing of the shear studs. Another important design aspect for C-PSW is the thickness of concrete panel. The concrete panel must be thick enough to ensure that global buckling of the steel plate does not occur prior to local buckling of the shear panel. AISC 341-10 [16] provides a recommendation of use of minimum of 200 mm concrete panel when the concrete panel is used in one side of the still infill plate, which is the case in this research. In this study, two equations based on classical buckling theory of stiffened plate are developed for determining shear stud spacing and thickness for the reinforced concrete panel. While AISC 341-10 [16] provides guidelines for the design and analysis of C-PSWs, currently there are no design guidelines available in CSA S16-09 [20] for design of this lateral load resisting system. More research is required for better understanding of the local and global behaviour of C-PSW before it can be adopted by the design code in Canada.

2. Nonlinear finite element model of composite plate shear walls

ABAQUS/Standard [21] with implicit formulation was used for all analysis purposes. 4-node doubly curved general purpose shell with reduced integration (ABAQUS shell element S4R) was used here to model the plate components of the C-PSW system namely, the steel infill plates, the steel boundary members and the reinforced concrete panels. The S4R element is based on an iso-parametric formulation. These elements possess six degree of freedom at each node: three translation and three rotations defined in its global co-ordinate system and are compatible with the damage plasticity model of

concrete used in this research. Usually, fish plates are used in practice to connect the infill plates to the boundary framing members. In the FE model, the fish plates were not modelled. Instead, infill plates were considered to be connected directly to the beams and columns. This assumption of neglecting the fish plate in FE model was shown to have negligible effect on the overall behaviour of SPSW [2]. In order to model the bolted connections between the RC panel and the steel infill plate, three dimensional 2-node linear beam elements (ABAQUS beam element B31) were used. The material properties (stress-strain curve with hardening) for the inelastic beam were adjusted in such a way that the global parameters, such as story drift, in-plane displacement, web and flange local buckling of beams, yielding of infill plates at different drift levels, and cracks at concrete layers from the experiment agree well with that from the finite element model.

Meshes were designed so as the steel plates, steel columns and steel beams have the common nodes at their junction. A bilinear elasto-plastic stress versus strain curve was adopted for steel beams, columns, and infill plates. Structural steel elements exhibit strain hardening with a post-yield stiffness approximately equal to 0.5–5% of the elastic stiffness [22]. For this study, a strain hardening of 2 percent of the elastic stiffness is considered for all analysis. The von Mises yield criterion was adopted for the all the analyses. The associated flow rule was used to obtain the plastic strain increment. In ABAQUS, both isotropic and kinematic strain hardening can be included in the finite element analysis. For the monotonic pushover analysis, a nonlinear isotropic hardening model was used as such a model is adequate for monotonic loading. For quasi-static cyclic loading and seismic loading that involves a significant number of strain and stress

reversals, the Bauschinger effect becomes important. Thus, for these two loading cases, a combined hardening rule was used in the analysis. The material property for the bolt steel was adopted from Kulak [23] based on the tension coupon test results for the specific grade of bolts used. The concrete was designed to have a minimum of 28 MPa. The concrete damaged plasticity model [24-25] available in ABAQUS, was found to be suitable for use where the concrete is subjected to monotonic, cyclic or dynamic loads. This damage plasticity model is capable of incorporating irreversible damage and can capture highly nonlinear behavior of concrete combined with stiffness degradation and stiffness recovery under load reversal.

The tensile stress-strain behavior was incorporated based on the concrete constitutive model for average stress-strain relation proposed by Belarbi and Hsu [26]. The tensile stress strain behavior takes into consideration the tension stiffening, strain-softening, and reinforcement interaction with concrete. To incorporate tension stiffening and strain softening in the FE model, tensile stress strain relationships were converted to tensile stress vs cracking strain and damage parameter vs cracking strain as shown in Fig. 1. The experimentally verified numerical constitutive model by Hsu and Hsu [27] is incorporated here in the damage plasticity model for describing the stress strain behavior of concrete in compression. First, compressive stress-strain relationships were converted to compressive stress vs inelastic strain and damage parameter vs inelastic strain, as shown in Fig. 2. In order to simulate the compressive behavior of reinforced concrete in concrete damaged plasticity model, the input provided were that of the Young's modulus 'E_c', the compressive stress 'σ_c' vs inelastic strain 'ε_c^{in}' relationship and the damage parameter value 'd_c' vs inelastic strain 'ε_c^{in}' relationship for the relevant grade and

constitutive model of concrete chosen. In the absence of sufficient data regarding the concrete used in experimentation, a compression stiffness recovery factor of '1' was used implying full compressive stiffness recovery upon crack closure as loading changes from tension to compression. A tension stiffness recovery factor of '0' was chosen assuming no tension stiffness recovery when the loading changes from compression to tension, once concrete crushing has been initiated. Further details of concrete damage plasticity model used in this paper can be found in [21, 28].

The dilation angle of a material can be obtained from a tri-axial compressive test and is defined as the ratio of the plastic volume change over plastic shear strain [29]. In this study, in the absence of sufficient information on the material properties of concrete used for the test of C-PSWs by Zhao and Astaneh-Asl [14] a realistic dilation angle value of 31^0 was chosen. This value has also been recommended in the literature [21]. In the FE model, reinforcement were modelled as a smeared layer in the RC panel.

3. Validation of finite element model

The finite element model (FEM) has been validated by comparing the results from available test. Very few experimental works have been reported using composite shear walls. In this study, the finite element model has been validated against the composite plate shear wall test conducted by Zhao and Astaneh-Asl [14]. Between their two test specimens, traditional and innovative C-PSWs, Zhao and Astaneh-Asl [14] reported that the innovative specimen behaved in a more ductile manner and also for the innovative system, damage to the concrete panel under relatively large cycles was much less in comparison to the traditional system. Thus, only the innovative test specimen, which had

32 mm gap between the edges of the concrete wall and the surrounding boundary steel frame, was considered in this research. The test specimen was a single bay structure with a steel moment resisting frame as the boundary members and composite shear walls embedded inside the moment resisting frame. The composite shear wall consisted of a steel plate shear wall and a reinforced concrete shear panel bolted to each other. The specimen was considered of three stories with the top and bottom panels of the specimen represented two half stories while the middle two panels represented two whole stories. Details of the test specimen can be obtained elsewhere [14].

The innovative C-PSW specimen was modeled in ABAQUS and a pushover analysis was carried out. The material properties were chosen as the one reported by the author's work like yield strength of boundary steel members as 350 MPa and that of infill steel plate as 248MPa. The concrete had a minimum f_c' of 28 MPa. A reinforcement ratio of 0.92% was maintained and 13 mm diameter A325 bolts were used to connect the reinforced concrete (RC) panels with the steel infill plate in accordance with the test specimen. As in the test, displacement loading has been applied through the center line of the top beam level. The displacement was increased to a maximum value as obtained from the envelope of hysteresis curve of physical test.

The element mesh of the composite plate shear wall is shown in Fig. 3(a). The measured (obtained from physical experimentation) and predicted (from FEA) base shear values are plotted against the overall story drifts in Fig. 3(b). The figure indicates that the finite element model predicts the initial stiffness and post-yield response of the shear wall very

well. The specimen behaved elastically up to overall drift levels of approximately 0.4%. At overall drift value of 0.6%, the experimental specimen showed yielding of all three horizontal beams and some yielding at column base. The finite element model (FEM) exhibited similar behavior at this drift level. At overall drift level of 1.2%, the experimental specimen developed local buckling and yielding in the infill steel plates. At drift level of 2.4%, the experimental middle and bottom beams started to form web and flange local buckling. Similar behavior was captured by the FEM at these drift levels.. The ultimate capacity of the specimen is under estimated by about 6%. The finite element model was also validated by comparing cyclic analysis results with the test results of the quasi-static cyclic test conducted by Zhao and Astaneh-Asl [14]. Hysteresis curves obtained from the finite element analysis were compared with the test results in Fig. 4. The hierarchical modes of failure and yielding of different components of the test specimen were compared with that of the finite element model and close correlation was observed. The slight differences between the results from the test and the FE model might be due to the small differences in the actual experimental set up and that of the FE model. Also, detailed stress-strain curves for the steel sections used in the test were not reported and only bilinear behavior of the steel materials was assumed.

Further validation of the finite element model was carried out by comparing cyclic analysis results with the test results of the quasi-static cyclic test conducted by Driver et al. [2]. Driver et al. [2] tested a four storey steel plate shear wall (similar to C-PSW, but without the concrete panel) under quasi-static cyclic loading. Details of the test specimen are available in the literature [2]. Hysteresis curves obtained from the finite element

analysis were compared with the test results in Fig. 5. In general, there is good agreement between the test results and the finite element analysis. Both the predicted capacity and stiffness of the SPSW are in excellent agreement with the test results. The hysteresis curves generated from FE analysis show slightly less pinching than that observed during the test.

One of the important factors for any seismic lateral load resisting system is the correct estimation of seismic response factor, R. In Canada, two different factors, R_d : ductility related force modification factor and R_0 : over-strength related force modification factor, are used in seismic design of structures (NBCC 2010). Researchers have so far proposed different methodologies for derivation of ductility related force modification factor. Newmark and Hall [31] derived a relationship between the ductility related force modification factor, R_d and the ductility ratio, μ according to the period of a structure.

$$R_d = \mu \text{ for } T > 0.5\,\text{s} \tag{1}$$

$$R_d = \sqrt{2\mu - 1} \text{ for } 0.1 < T < 0.5\,\text{s} \tag{2}$$

$$R_d = 1 \text{ for } T < 0.03\,\text{s} \tag{3}$$

Ductility ratio of a structure, μ, is defined as ratio of maximum lateral displacement (Δ_{max}) or displacement at failure to lateral displacement at yield (Δ_y).

$$\mu = \frac{\Delta_{\max}}{\Delta_y} \tag{4}$$

Thus, in order to obtain ductility of a structural system, it is important to identify yield and maximum displacements of the structure from a force deformation relationship. Park

(1988) proposed that displacement corresponding to first significant yielding could be considered as the yield displacement of the structure. It was also suggested that displacement corresponding to the post-peak displacement when the load carrying capacity undergoes a small reduction (often taken as 10%-20%) might be considered as the maximum displacement of the structure [32]. The suggestions made by Park (1988) are considered in this study. Test based ductility related force modification factor was estimated from the force deformation relations of both traditional and innovative C-PSWs tested by Zhao and Astaneh-Asl [14]. Figure 6 presents the cyclic envelopes of the two specimen tested by Zhao and Astaneh-Asl [14]. For both specimens the overall drift value of 0.006 rad was established as the ‘‘Significant Yield Point’’ as at this drift level, some yield lines appeared on the beams as well as in the column bases. Shear strength of the innovative specimen dropped to about 80% of the maximum shear strength of the specimen at an overall drift level of 0.044 rad, and the specimen was considered failed. In case of traditional C-PSW, test showed that the strength dropped to about 80% of the ultimate shear strength at a drift level of 0.042 rad. These values (0.044 rad and 0.042 rad) of overall drift levels, as indicated in Fig. 6, were considered the maximum overall drifts to reach “Points of Maximum Ductility.” Using the relation between maximum drift to yield drift as presented in Eq. (4), the overall ductility values for Innovative and Traditional C-PSW specimens were calculated as 7.33 and 7.0 respectively. Assuming that the natural periods of vibration of the 4-storey and 6-storeyC-PSWs studied in this research greater than 0.50 s, which is verified later from frequency analysis, the R_d values could be selected for the selected C-PSWs with Eq. (1). In the current edition of National Building Code of Canada (NBCC 2010), R_d factor ranges from 1.0 for brittle systems

such as unreinforced masonry to 5.0 for the most ductile systems. It is believed that this range is realistic for building structures (Park and Paulay 1975; Paulay and Priestley 1992). NBCC 2010 [30] and CSA S16-09 [20] assign the highest ductility related force modification factor, R_d of 5.0, to ductile SPSW. In both SPSW and C-PSW, the hierarchical modes of failure and yielding are same: steel infill plate yielding is considered as the main ductile fuse, followed by yielding at the end of steel beams and finally plastic hinging at the base of columns. Thus, based on the results of the test program by Zhao and Astaneh-Asl [14] and in the absence of any provision for C-PSW in Canada, similar to the provision for ductile SPSW, a ductility related force modification factor, R_d of 5.0 is used for design of C-PSWs.

4. Seismic design of composite plate shear walls

4.1 Selection of composite plate shear walls

The buildings considered here for seismic analysis are one 4-storey and one 6-storey hypothetical office building located in Vancouver having a plan area of $2014\,\mathrm{m}^2$. Figure 7(a) shows typical floor plan of the hypothetical buildings considered for seismic analysis. As shown in the plan, each of the buildings has two identical C-PSWs to resist lateral forces in each direction, thus, each composite shear wall will resist half of the design seismic loads. Only innovative C-PSW system was considered in this study. The C-PSW under consideration for seismic analysis is designated as C-PSW1. For simplicity, torsion was neglected. Each C-PSW was 3.8m wide, measured from center to center of columns, and had an aspect ratio of 1.0 (storey height of 3.8m). Thus, the 4-storey building had a total height of 15.2 m and the 6-storey building had a total height of

22.8 m. The buildings were assumed to be founded on very dense soil or soft rock (site class C according to NBCC 2010). A dead load of 4.26 kPa for each floor and 1.12 kPa for the roof were used. The live load on all floors was taken as 2.4 kPa and no live load was considered at the roof level. NBC 2010 [30] recommends use of load combination '1.0 D + 1.0 E + 0.5 L or 0.25 S' (where, D = dead load, L = live load, S = snow load, and E = earthquake load) when earthquake load is present. Thus, load combination 'D + 0.5L + E' was considered for floors and for the roof, the load combination 'D + 0.25S + E' was considered. A steel plate thickness of 4.8 mm was used as the minimum practical thickness based on requirements to be bolted with the reinforced concrete panels and handling issues. 13 mm diameter A325 bolts were selected for connecting the steel infill plate with the RC panel.

4.2 Design of composite plate shear walls

In order to design the C-PSWs, the equivalent static force method was employed to find out the storey shear forces at each storey according to NBCC 2010 [30]. The design seismic base shear (V) calculated according to NBCC 2010 is as follows:

$$V = \frac{S(T_a)M_V I_E W}{R_d R_0} \geq \frac{S(2.0)M_V I_E W}{R_d R_0} \tag{5}$$

where $S(T_a)$ is the spectral acceleration; M_V is an amplification factor accounting for higher mode effects on base shear; I_E is the importance factor for the structure; W denotes the total dead load in addition to 25% of the snow load; similar to ductile SPSW an over strength force modification factor R_0 of 1.6 was used in the design of C-PSW.

According to the NBCC 2010, for structures having R_d greater than 1.5 the design base shear should assume a maximum value as:

$$V \leq \frac{2S(0.2)I_E W}{3R_d R_0} \tag{6}$$

The final base shear calculated was distributed at each storey of the structure as:

$$F_X = (V - F_t)\frac{W_X h_X}{\sum_{i=1}^{i=n} W_i h_i} \tag{7}$$

where F_t is an extra lateral force component applicable to the top floor; W_i or W_X denotes the dead load in addition to 25% snow load applicable to the storey i or x and h_x or h_i denotes the height from the base to the storey level i or x respectively. The equivalent static lateral forces determined based on the NBCC 2010 for the 4- storey C-PSW were 152.5 kN, 305.1 kN, 457.7 kN and 206.3 kN for the first storey, second storey, third storey and roof respectively. The lateral forces determined for the 6- storey C-PSW were 104.2 kN, 208.4 kN, 312.6 kN, 416.8 kN, 521.1 kN and 211.3 kN for the first storey, second storey, third storey, fourth storey, fifth storey and roof respectively. AISC 341-10 [16] requires that the steel infill plates of C-PSWs be designed as the main energy dissipating elements. The design shear strength of the plate is based on the shear yielding of the stiffened steel plate and is given by:

$$V_r = \phi 0.6 A_{sp} F_y \tag{8}$$

where $\phi = 0.9$; A_{sp} is the horizontal area of the stiffened steel plate; F_y is the specified yield stress of the steel plate

Thus, the steel infill plates can be selected to resist the total seismic load calculated using equivalent lateral force method in NBCC 2010. As per the capacity design method in AISC 341-10 [16], the beams and columns of the C-PSW shall be designed for the expected strength of the steel infill plates in shear, $0.6A_{sp}R_yF_y$, where $R_y = 1.1$ and the beams and columns adjacent to the composite webs shall be designed to remain essentially elastic under the maximum forces that is developed by the fully yielded steel infill plates, except that plastic hinging at the ends of beams is allowed. Also, plastic hinges are allowed at base of the boundary columns.

Boundary members for the C-PSW were designed according to the capacity design approach similar to what was proposed by Berman and Bruneau [35] for ductile SPSW. AISC 341-10 recommends adequate stiffening of the steel infill plate by encasement of the steel plate or attachment with a RC panel. The concrete panel was selected as per provisions of AISC 341-10, which was selected to be of 200 mm thickness and reinforcement ratio of 0.0025 was maintained with the bar spacing not exceeding 450 mm to comply with the minimum requirements. A shear stud spacing of 300 mm was selected for all the C-PSWs. The shear stud spacing and the thickness of reinforced concrete panel used for the C-PSWs were also checked based on the equations, developed later using the concepts of classical buckling theory of stiffened steel plate. The selected C-PSWs are shown in Fig. 8.

5. Non-linear dynamic analyses of composite plate shear walls

5.1 FE model and initial conditions

The selected C-PSWs were modelled in ABAQUS. A mesh sensitivity study was conducted in order to help determine the effect of mesh size on the performance and behavior of the C-PSWs. Element dimensions were varied from 80 mm to 300 mm at the steel plate region and suitably at the boundary elements based on the dimension available. It was observed that the mesh size in the above range did not affect the local or global performance of the C-PSWs. Hence, a mesh of approximately 300 mm in element dimension at the steel infill plate region was used for the nonlinear dynamic analysis.

The nominal yield strength of steel infill plates, boundary columns and beams were selected as 350 MPa and all steel members were assumed to have a modulus of elasticity of 200 000 MPa. The concrete was selected to have compressive as well as tensile damage and had a compressive strength of 28 MPa. Frequency analyses for the C-PSWs were carried out prior to seismic analyses to find out the fundamental mode shapes and frequencies for the C-PSWs. A dummy gravity column was incorporated into the finite element model to take account of P-Δ effects. Figure 9 presents analytical model for 4-storey C-PSW. In this model, the gravity column was made of 2-node linear 3-D truss (ABAQUS element T2D3) elements and was connected with the C-PSW at every floor with pin ended rigid link connections. Thus, at each floor, the horizontal degree of freedom of the gravity column was constrained to be the same as that of the C-PSW to maintain displacement compatibility of structural members interacting through rigid floor diaphragms. The gravity column was designed so as not to provide any lateral stiffness and it carried half of the total remaining mass of the building since there are two C-PSWs in each mutually perpendicular directions of the building plan. From frequency analyses,

the first two mode periods (in-plane) of the 4-storey C-PSW (aspect ratio 1.0) were obtained as 0.63 s and 0.20 s respectively. For 6-storey C-PSW, the first two in-plane periods were 1.16 s and 0.31 s respectively. These periods were used to determine Rayleigh proportional damping constants for 4-storey and 6-storey C-PSWs. A 5% Rayleigh proportional damping was assumed in the first two modes of vibration, which included a cumulative modal mass equal to more than 90% of the total mass applied on the C-PSW.

5.2 Selection and scaling of ground motion

National Building Code of Canada (NBCC 2010) prescribes input earthquake ground motions in terms of a Uniform Hazard Spectrum (UHS) having a 2% chance of being exceeded in 50 years. The target UHS is also specified for a number of standard site conditions. NBCC 2010 also emphasizes the use of spectrum compatible earthquake records to be used for seismic analysis. The building considered here being located at Vancouver, the uniform hazard spectrum for Vancouver provided in NBCC 2010 has been used in this research. ASCE 7-10 [36] recommends a minimum of three ground motion records for time history analysis, when peak maximum response are considered for component checking and a minimum of seven ground motion records when the average of maximum response are considered for component checking.

In this research, eight ground motion records have been selected and used for time history analysis: four real ground motion records from the strong ground motion database of Pacific Earthquake Engineering Research Center [37] and four simulated earthquake records from Engineering Seismology toolbox website [38]. Table 1 and Table 2 present

some important features of the four real ground motion record and four simulated earthquake records. The selected real ground motions were chosen to have A/V (A, peak acceleration in scale of g and V, peak velocity in m/s, where g is acceleration due to gravity in m/s^2) values close to 1 conforming with the A/V value for an earthquake expected in Vancouver [39]. Only horizontal component of the ground motions were considered. The simulated earthquakes included two different sets of records having magnitude 6.5 and 7.5 respectively for soil class C.

The selected ground motions were scaled based on the partial area method [39] of ground motion scaling. According to this method, the area under the acceleration response spectrum curve of the selected ground motion and design response spectrum are compared and made equal by finding out a suitable scaling factor. Area under the acceleration response spectrum curves of ground motion records between 0.2T to 1.5T; where, T is the fundamental period of vibration of the building, is compared with the area under the design response spectrum of Vancouver in the designated range and made equal by finding out a suitable scaling factor and modifying the concerned accelerogram with that factor. This period range of the excitation motions is assumed to have the largest effects on the structural response. Scaling factors for all the selected earthquakes were calculated and are provided in Table 1 and Table 2. Figures 10 (a) and 10(b) show the response spectra for the eight selected scaled seismic records along with design spectrum of Vancouver determined from the spectral acceleration values available in NBCC 2010. It is observed that, for both 4-storey and 6-storey C-PSWs, the average of all the response spectra does not fall below the design response spectrum in the period range from 0.2T to 1.5T, where T is the fundamental period of the selected C-PSWs.

5.3 Seismic response of C-PSWs

Non-linear time history analyses were performed in ABAQUS. Under all earthquake records, the 4-storey C-PSW behaved in a stable and ductile manner. The RC-panels were capable of successfully restraining out-of-plane motion of the steel infills and were undamaged under all ground motions except for one record (San Fernando earthquake), where minor damage was identified at the first storey. Figure 11 presents the average peak storey shears for 4-storey and 6-storey C-PSWs under the selected artificial and real ground motions and the contributions by the various components of the C-PSWs: namely, the steel infill, boundary columns and the RC panel. For 4-storey C-PSW under simulated earthquake records, the maximum base shear was found as 5390 kN, obtained for 6C2 earthquake record. The peak storey shear contributions by the boundary columns and the RC panel at the base, for 6C2 record, were 27% and 10% respectively. As observed from Fig. 11, for 4-storey C-PSW under simulated earthquake records, the average shear contributions by the columns and the RC panel at the base, are 23.5% and 10% respectively. Storey shear percentage contributions by the RC-panels for higher stories were observed to be practically insignificant. For the 4-storey C-PSW, under real earthquake records, the maximum base shear was found as 5170 kN for Imperial Valley 2 record. For this earthquake record, the storey shear contributions at the base by the boundary columns and the RC panel were observed as 25% and 10% respectively. Figure 11 also shows that, for 4-storey C-PSW under real earthquake records, the average shear contributions from the columns and the RC panel at the base, are 22% and 10.8% respectively. For 4-storey C-PSW, for all ground motions, steel infill plates for the first and second storey fully yielded. This is also observed from Fig. 11 as the average

dynamic shears for the bottom two storeys of 4-storey C-PSW are very close to the nominal shear strength of the plate web, 3353 kN, as calculated by Eq. (8).

The 6-storey C-PSW also behaved in a ductile and stable manner. For all the earthquake records except for 7C2 earthquake record, steel infill plates of the bottom three floors were yielded. Yielding in infill plates occurred when the dynamic shears reached or exceeded the nominal shear strength of the plate web of 6-storey C-PSW, 3312 kN, as calculated by Eq. (8). For 7C2 earthquake record infill plate at the fourth floor also yielded. Figure 11 presents the average peak storey shears for 6-storey C-PSW under the selected ground motions. The maximum dynamic base shear was found as 5313 kN, obtained for 7C1 earthquake record. The peak storey shear contributions by the boundary columns (observed for 7C1 record) and the RC panel (observed for 7C2 record) at the base were 29% and 8.5% respectively. As observed from Fig. 11, for 6-storey C-PSW under simulated earthquake records, the average shear contributions by the columns and the RC panel at the base, are 26% and 6% respectively. Similar to 4-storey C-PSW, storey shears taken by the RC-panels in higher stories were very small. For the 6-storey C-PSW, under real earthquake records, the maximum base shear was found as 5285 kN for Imperial Valley 2 earthquake record. For this earthquake record, the storey shear contributions at the base by the boundary columns and the RC panel were observed as 26% and 9.5% respectively. Fig. 11 also shows that, for 6-storey C-PSW under real earthquake records, the average shear contributions from the columns and the RC panel at the base are 21% and 8.5% respectively.

It can be clearly observed from Fig. 11 that NBCC 2010 static base and storey shear forces calculated are much lower than those from seismic analysis. This is mainly due to the over strength in the C-PSWs caused by the use of thicker steel plates than required due to handling and practical requirements. Also, a significant portion of shear is taken by boundary columns and reinforced concrete panels, which is not considered in the current design approach of C-PSW since total shear is assumed to be resisted by the steel infill plates only.

For some cases, very small partial yielding was observed in the outer flanges of steel boundary columns at the base, thereby achieving design objective of C-PSW to sustain the full yield force from the steel infill plates. For the 6-storey C-PSW, RC-panels were essentially undamaged except for two earthquake records (Imperial Valley 2 and San Fernando earthquakes) where small amount of micro-cracking was observed. Microcracks were concluded based on plastic strain in tension (ABAQUS PEEQT) output values corresponding to concrete strain in tension beyond the point of maximum tensile strength based on the Belarbi and Hsu [26] concrete constitutive model in tension.

Figures 12 and 13 present the envelopes of absolute maximum column axial forces and column moments obtained from the seismic analyses of 4-storey C-PSW and 6-storey C-PSW respectively. It is observed that, for all ground motions, the axial forces in all floors are lower than the design axial forces obtained from the capacity design method. The maximum column axial force (as shown in Fig. 12) obtained at the base from the time history analyses, 13499 kN for the Kobe 1995 earthquake record, is 19.5% lower than

the design axial force, 16766 kN. For the 6-storey C-PSW, the maximum column axial force (as shown in Fig. 13) at the base from the time history analyses, 20946 kN for the artificial 7c2 earthquake record, is 12% lower than the design axial force, 23848 kN. Figure 12 also shows that the peak seismic demand for flexure at the base of the columns of 4-storey C-PSW, 875 kN·m for Kobe 1995 earthquake record is lower than the design moment of 2138 kN·m. For the 6-storey C-PSW (as shown in Fig. 13), the peak seismic demand for flexure at the base of the columns, 1013 kN·m for Imperial Valley 1 earthquake record, is lower than the design moment of 2138 kN·m. Also, for both selected C-PSWs, the design column moments for the upper stories are larger than the column moments determined from the seismic analyses. This occurs because of the assumption made in the capacity design method that all the steel web plates are fully yielded. Though AISC 341-10 [16] permits plastic hinges to be formed at the end of the beams of C-PSW, plastic hinges were not observed to form at the end of beams at top floors during the seismic analyses of the C-PSWs. Thus, design column moments obtained from capacity design method were found to be conservative.

Figure 14 shows (the critical portion is only presented) the extent of yielding in the bottom four storeys of the 6-storey C-PSW and bottom two storeys for the 4-storey C-PSW, when the base shear is at its maximum value for 7c2 earthquake record. It is observed that yielding is mainly in the first four infill plates for 6-storey C-PSW and first two infill plates for the 4-storey C-PSW. There was some yielding at the ends of beams, at first and second storeys, for 6-storey shear wall. For the 4-storey C-PSW, yielding at the ends of beams was observed at the first floor only. Figures 15 and 16 present the peak

interstorey drifts in every storey obtained from the seismic analyses for the set of ground motions chosen. It was found that the interstorey drifts are within the allowable range of NBCC 2010.

6. Evaluation of code period formula for C-PSWs

In order to evaluate the code based formula for estimating fundamental periods of C-PSWs, a total of eight buildings with C-PSWs as lateral load resisting system were considered. They consisted of two sets of buildings with different symmetrical floor plans having C-PSWs of aspect ratio of 1.0 and 1.5 respectively. The floor plans are shown in Fig. 7. For each set of floor plan, 1-storey, 2-storey, 4-storey and 6-storey buildings were considered. The buildings for these C-PSWs were chosen to be hypothetical office buildings in Vancouver founded on soft rock (site class C according to NBCC 2010) and having plan area of 2014 m^2 and consisting of two identical shear walls to resist lateral forces in each direction. Table 3 presents the final columns and beams for the selected C-PSWs.

The building codes namely the NBCC 2010 [30] and ASCE 7-10 [36] specify upper limits on fundamental periods calculated based on simple methods of structural analysis in order to limit the values of design seismic loads that are too low due to modelling assumptions. NBCC 2010 specifies that, for shear walls, periods calculated by any analytical method should not exceed 2.0 times the value determined by Eq. (9). ASCE 7-10 [36] standard limits the upper limit of fundamental periods as 1.4 times the value for high seismic zones to 1.7 times the value for low seismic zones, as determined by Eq. (9).

$$T = C_t h^x \tag{9}$$

where, T is the fundamental period of the structure, h is the height of the structure above the base, C_t and x are constants. NBCC 2010 and ASCE 7-10 recommend values of C_t as 0.05 and x as 0.75 for shear walls. An eigenvalue extraction technique was used to calculate the natural frequencies and the corresponding mode shapes of C-PSWs. Figure 17 compares the code predicted period formula with the computed fundamental periods obtained from the detailed finite element analyses. The overall results suggest that the code based periods provide conservative estimates of fundamental periods for C-PSWs, leading to higher seismic forces. Studies also show that code building periods are intentionally shorter than the mean values to be on the conservative side for the estimate of design forces. The constants C_t and x are determined by linear regression of the numerical analysis period data, as was done by Goel and Chopra [40] for moment resisting frame. From a least square regression analysis of the available C-PSW periods, the resulting expression to represent the best-fit to the period data of C-PSWs is obtained as

$$T = 0.019h^{1.24} \tag{10}$$

One of the assumption in the derivation of the constants for code period formula is that the base shear is proportional to $1/T^{\gamma}$. The value of γ is bounded between 0 to 1 [40], giving a recommended value of x between 0.5 and 1.0 for Eq. (9). For different values of x, constrained regression analyses can be conducted to determine C_t [40]. Consistent with the code period formula for C-PSW, for this study, constrained regression analysis was conducted for a fixed x value of 0.75. From constrained regression analysis, for a fixed x value of 0.75, the associated C_t value of 0.066 is obtained. For seismic design

purposes, the estimate of the natural period needs to be a conservative value. This can be obtained by lowering the best-fit line, for x = 0.75, by one standard deviation. Thus the proposed formula for C-PSWs is:

$$T_{\text{propose}} = 0.043 h^{0.75} \tag{11}$$

The proposed period formula for C-PSW is also presented in Fig. 17. It is observed from Fig. 17 that only one data point fall slightly below the proposed period equation.

7. Determination of equations for shear stud spacing and concrete panel thickness

Currently there are no guidelines for minimum or maximum spacing of the shear studs and the thickness of concrete panel to be used for C-PSWs in the Canadian standard. The concrete panel must be thick enough to ensure that global buckling of the steel plate does not occur prior to local buckling of the shear panel. AISC 341-10 [16] provides a recommendation of use of minimum of 200 mm concrete panel when the concrete panel is used in one side of the still infill plate, which is the case in this research. This section presents a rational method for determining shear stud spacing and thickness for the reinforced concrete panel. The method is based on classical buckling theory of stiffened steel plate.

The concrete panel must be connected with the steel infill plate in such a way that steel plate reaches to yield prior to overall or local buckling. This requirement is used to calculate the minimum shear stud spacing of C-PSWs. When a plate is subjected to a state of pure shear, the critical shear buckling stress can be obtained as:

$$\tau_{cl} = K_{Sl} \frac{\pi^2 E}{12\left(1-\nu^2\right)\left(\frac{b}{t}\right)^2} \tag{12}$$

where K_{Sl} is the buckling coefficient for shear buckling stress; b is the width of the steel plate; t is the plate thickness; E is the modulus of elasticity of steel plate; and ν is the Poisson's ratio of steel plate .

Critical stress coefficients, K_{Sl}, for plates subjected to pure shear have been evaluated when the plate is clamped (edges restrained from out-of-plane rotation). For finite-length rectangular plate with clamped edges, Moheit [41] provides following expressions for K_{Sl} :

$$K_{Sl} = 5.6 + \frac{8.98}{\alpha^2} \text{ for } \alpha \le 1 \quad (13)$$

$$K_{Sl} = 8.98 + \frac{5.6}{\alpha^2} \text{ for } \alpha \ge 1 \quad (14)$$

where $\alpha = \frac{b}{d}$, d and b are two sides of rectangular plate with side d is shorter side

AISC 341-10 [16] requires that steel plates of C-PSWs fail in yielding rather than buckling. Thus, the corresponding critical buckling stress should be greater than the yield stress. One approach to do this is to transform the concrete wall to vertical and horizontal stiffeners along the shear stud lines, as shown in Fig. 18. Buckling of each sub panel can then be checked using elastic buckling theory considering steel connectors as fixed plate support points [16, 42]. As seen in Fig. 18, the distance between vertical stiffeners (distance between vertical shear stud lines) is C_1, whereas, the distance between horizontal stiffeners is C_2. The shear studs are assumed to have a diameter of D.

Assuming equal spacing for vertical and horizontal stiffeners, that is $C_1 = C_2 = c$, the elastic critical shear buckling stress, τ_{crl}, for local buckling of a typical subpanel (surrounded by horizontal and vertical shear stud lines) is obtained as:

$$\tau_{crl} = K_{Sl} \frac{\pi^2 E}{12\left(1-\nu^2\right)\left(\frac{c}{t}\right)^2} \tag{15}$$

where c is the spacing between the stiffeners.

For a typical C-PSW, where the spacing of vertical and horizontal stiffeners are same, $\alpha = 1$, and $K_{Sl} = 14.58$. As stated in AISC 341-10 [16], shear studs must be spaced in as such that local buckling of each sub panel only occurs once the panel yields in shear. Thus,

$$\tau_{crl} \geq \tau_{sy} \tag{16}$$

where τ_{sy} is shear yield stress of the steel infill plate, which is equal to $\frac{\sigma_y}{\sqrt{3}}$ with σ_y yield strength of the steel infill plate. Thus Eq. (15) becomes:

$$14.58 \frac{\pi^2 E}{12\left(1-\nu^2\right)\left(\frac{c}{t}\right)^2} \geq \frac{\sigma_y}{\sqrt{3}} \tag{17}$$

$$c \leq \sqrt{\frac{20.77 E t^2}{\sigma_y \left(1-\nu^2\right)}} \tag{18}$$

Equation (18) defines the maximum shear stud spacing that can be used to avoid any local buckling in the sub panel of C-PSW. For typical values of E and ν for steel, (E = 200,00 MPa and ν = 0.3), Eq. (18) becomes:

$$c \leq 2136.5 t \left(\sigma_y\right)^{-\frac{1}{2}} \tag{19}$$

For the selected C-PSWs ($t = 4.8\,\text{mm}$ and $\sigma_y = 350\,\text{MPa}$), the maximum shear stud spacing can be calculated as 548 mm, which is higher than the shear stud spacing (300 mm) used in this research.

AISC 341-10 [16] recommends that the thickness of the concrete encasement should be calculated to make sure that local buckling occurs in the sub panel instead of global buckling mode of the full C-PSW. Exact solutions for long orthotropic simply supported plates in shear [15, 43] were used here to find out the critical shear stress for global buckling, τ_{crg}. The shear stress for global buckling for closely spaced stiffeners is:

$$\tau_{crg} = \frac{K_{Sg}\pi^2}{d^2 t}\left(D_x\right)^{\frac{3}{4}}\left(D_y\right)^{\frac{1}{4}} \tag{20}$$

where K_{Sg} is the global buckling factor, which is a function of D_x, D_y, C_1, C_2, as well as the steel plate boundary conditions. The minimum values of K_{Sg} for plate to frame connection with pinned and rigid connections are 3.64 and 6.9 respectively.

D_x = flexural stiffness for bending about x-axis

$$D_x = \frac{EI_x}{C_1} + \frac{Et^3}{12\left(1-\nu^2\right)} \tag{21}$$

D_y = flexural stiffness for bending about y-axis

$$D_y = \frac{EI_y}{C_2} + \frac{Et^3}{12\left(1-\nu^2\right)} \tag{22}$$

To make sure that local buckling mode occurs instead of global buckling, following condition must be satisfied:

$$\tau_{crg} > \tau_{crl} \tag{23}$$

The vertical and horizontal stiffeners are assumed to have the same moment of inertia and the stiffeners are assumed to be equally spaced. The above criteria leads to the expression as follows:

$$h > 0.65t\left[\frac{K_{Sl}d^2n}{K_{Sg}cD} - \frac{cn}{D}\right]^{1/3} \tag{24}$$

For a concrete panel with thickness of h; shear stud diameter of D; modular ratio of n, using a minimum value of 3.64 for global buckling K_{Sg} to obtain conservative estimate of concrete panel thickness and a conservative K_{Sl} value of 14.58 when horizontal and vertical shear studs have same spacing, the concrete panel thickness is calculated as 155 mm, which is less than the minimum required concrete panel thickness used in this research.

8. Summary and conclusions

Nonlinear seismic analyses under earthquake ground motions typical of Western Canada were performed to evaluate the performance a typical 4-storey and 6-storey composite plate shear wall. The analyses provided information on the shear and flexural demand on the lateral load resisting system. The key findings from this study are as follows:

(1) The finite element model developed was found to provide excellent correlation with the experimental specimen in quasi-static pushover and cyclic analysis. The model captured all essential behavioral features of the test specimen analysed.

(2) The 4-storey and 6-storey C-PSW finite element specimens analysed under a set of eight strong earthquake records were found to provide excellent structural performance in terms of stiffness, ductility, and high shear strength accompanied by minimal damage in

terms of concrete cracking and crushing. It was observed from the seismic analyses that the boundary columns and RC-panel together can contribute towards a significant amount of shear strength, as much as 30% (more than 20% of total shear strength is resisted by columns), which is ignored in the current AISC 341-10. This shall be acknowledged in the current code and as such, beams at every storey of C-PSW must have sufficient flexural resistance such that at least 20% of the applied factored storey shear force can be resisted by the boundary moment resisting frame.

(3) No plastic hinges were formed at the boundary columns, which were capacity designed. Design column moments and axial forces were shown to agree well with the results from the nonlinear seismic analyses of the selected C-PSWs, while providing slightly conservative results.

(4) The interstorey drifts obtained from the nonlinear time history analyses were well within the NBC 2010 limit of 2.5% of the interstorey height.

(5) It can be observed from the frequency analyses of the selected C-PSWs that the current code formula predicts periods that are generally shorter than those obtained from detailed finite element analysis.

(6) The proposed formula for determining fundamental periods for C-PSWs, $T_{\text{propose}}=0.043h^{0.75}$, which is based on a regression analysis, is very simple and convenient for engineering design applications. It is recognised that the proposed period formula derived in this study is based on the stiffness of the C-PSW alone. With stiffness contributions from other structural and non-structural components in the building, the period will become slightly shorter. Also, the proposed equation is derived with a limited period data. It is thus suggested that the proposed formula be re-evaluated should field

measurements of periods on C-PSW buildings or additional data from frequency analysis of more C-PSWs become available.

(7) Finally, two equations were developed for the determination of shear stud spacing and minimum reinforced concrete panel thickness. The equations are simple and easy to use for design of composite plate shear walls. However, a detailed experimental and analytical investigation is required before these equations can be adopted by the code.

It is acknowledged that the applicability of the seismic force reduction factor of 5.0 for C-PSW needs to be verified through nonlinear dynamic time history analyses of several representative multistorey C-PSW buildings with a wide range of building heights, bay widths, and seismic design categories following the approach adopted from the FEMA P695- methodology on the quantification of building seismic performance factors.

Acknowledgements

Funding for this research project is provided by the Faculty of Engineering and Computer Science, Concordia University, Montreal, Canada and the Natural Sciences and Engineering Research Council of Canada. Their support is gratefully acknowledged.

References

[1] Timler, P.A., and Kulak, G.L. Experimental study of steel plate shear walls. Structural Engineering Report No. 114, Dept. of Civil Engineering, University of Alberta, Edmonton, AB; 1983.

[2] Driver, R.G., Kulak, G.L., Kennedy, D.J.L., and Elwi, A.E. Seismic behaviour of steel plate shear walls." Structural Engineering Report No. 215, Department of Civil and Environmental Engineering, University of Alberta, Edmonton, Canada; 1997.

[3] Lubell, A.S., Prion, H.G.L., Ventura, C.E., and Rezai, M. Unstiffened steel plate Shear Wall performance Under Cyclic Load. Journal of Structural Engineering, ASCE 2000; **126**(4): 453-460.

[4] Berman, J. W., and Bruneau, M. Experimental investigation of light-gauge steel plate shear walls. ASCE Journal of Structural Engineering 2005;131(2):259-267.

[5] Vian, D. Steel plate shear walls for seismic design and retrofit of building structures. PhD dissertation, State Univ. of New York at Buffalo, Buffalo, N.Y.; 2005.

[6] Guo L, Rong Q, Ma X, Zhang S. Behavior of steel plate shear wall connected to frame beams only. Int J Steel Struct 2011;11(4):467–79.

[7] Sabouri-Ghomi S, Sajjadi SRA. Experimental and theoretical studies of steel shear walls with and without stiffeners. J Constr Steel Res 2012; 75:152–159.

[8] Thorburn LJ, Kulak GL, Montgomery CJ. Analysis of steel plate shear walls. Structual Engineering Report 107. Edmonton, Alberta, Canada: Dept. of Civil Engineering, University of Alberta; 1983.

[9] Berman JW, Bruneau M. Capacity design of vertical boundary elements in steel plate shear walls. Eng J, 2008; 45(1):57–71.

[10] Bhowmick, A. K., Driver, R. G., and Grondin, G. Y. Nonlinear Seismic Analysis of Steel Plate Shear Walls Considering Strain Rate and P-Delta Effects." Journal of Constructional Steel Research 2008, 65 (5):1149-1159.

[11] Topkaya CA, Kurban CO. Natural periods of steel plate shear wall systems. J Constr

Steel Res 2009; 65(3):542–51.

[12] Qu B, Bruneau M. Capacity design of intermediate horizontal boundary elements of steel plate shear walls. J Struct Eng 2010;136(6):665–75.

[13] Ghosh S, Kharmale SB. Research on steel plate shear wall: past, present and future. In: Becker LM, editor. Structural steel and castings: shapes and standards, properties and applications. Hauppauge, USA: Nova Science Publishers Inc.; 2010.

[14] Zhao, Q. and Astaneh-Asl, A. Cyclic Behavior of Traditional and Innovative Composite Shear Walls. ASCE Journal of Structural Engineering 2004; 130(2):271-284.

[15] Allen, H.G. and Bulson, P.S. Background to Buckling. McGraw Hill Book Company, U.K. 1980.

[16] AISC 341-10. Seismic provisions for structural steel buildings. American Institute of Steel Construction, Chicago, IL, 2010.

[17] Guo L, Ma X, Li R, Zhang S. Experimental research on seismic behavior of C-SPSWs connected to frame beams. Earthquake Engineering and Engineering Vibration 2011; 1:65–73.

[18] Guo LH, Li R, Rong Q, Zhang S. Cyclic behavior of SPSW and CSPSW in composite frame, Thin Walled Structures 2012; 51:39-52.

[19] Rahai, A., and Hatami, F. Evaluation of composite shear wall behaviour under cyclic loadings. Journal of Constructional Steel Research 2009; 65:1528–1537.

[20] Canadian Standards Association, CAN/CSA-S16-09. Limit States Design of Steel Structures. Toronto, Ontario, Canada, 2009.

[21] Hibbitt, Karlsson, and Sorensen. ABAQUS/Standard User's Manual. Version 6.11, HKS Inc., Pawtucket, RI; 2011.

[22] Saatcioglu, M., and Humar, J. Dynamic analysis of buildings for earthquake resistant design. Canadian Journal of Civil Engineering 2003; 30: 338–359.

[23] Kulak, G. L. High Strength Bolting for Canadian Engineers. Canadian Institute of Steel Construction, 2005.

[24] Lubliner, J., Oliver, J., Oller, S. and Onate, E. 1989. A Plastic-Damage Model for Concrete. International Journal of Solids and Structures 1989; 25(3): 299-326.

[25] Lee, J., and Fenves, G. L. Plastic-Damage Model for Cyclic Loading of Concrete Structure. Journal of Engineering Mechanics, ASCE 1998, 124(8): 892-900.

[26] Belarbi, H., and Hsu, C.T.T. Constitutive laws of concrete in tension and reinforcing bars stiffened by concrete. ACI Structural Journal 1994; 91(4): 465–474.

[27] Hsu, L.S., and Hsu, C.T.T. Complete stress-strain behaviour of high-strength concrete under compression. Magazine of Concrete Research 1994; 46(169): 301-312.

[28] Dey, S. Seismic performance of Composite Plate Shear Walls. M.A.Sc. Thesis, Concordia University, Montreal, Canada; 2014.

[29] Venneer. P. A. & de Borst, R. Non-associated plasticity for soils, concrete and rock. Heron 1984; 29, No.3.

[30] NBCC. National Building Code of Canada. National Research Council of Canada (NRCC), Ottawa, ON, Canada, 2010.

[31] Newmark, N.M., and Hall, W.J. Earthquake spectra and design. Engineering Monograph MNO-3, Earthquake Engineering Research Institute (EERI), Berkeley, California, 1982.

[32] Park, R. Ductility evaluation from laboratory and analytical testing. Proceedings of the 9th World Conference on earthquake Engineering, Tokyo, Japan, 1988, pp.605-616.

[33] Park, R., and Paulay, T. Reinforced concrete structures. John Wiley & Sons, New York, 1975.

[34] Paulay, T., and Priestley, M.J.N. Seismic design of reinforced concrete and masonry buildings. John Wiley & Sons, New York, 1992.

[35] Berman J.W. and Bruneau M. Capacity Design of Vertical Boundary Elements in Steel Plate Shear Walls. Engineering Journal 2008; First Quarter: 57–71.

[36] ASCE 7-10. Minimum Design Loads for Buildings and Other Structures. American Society of Civil Engineers, Reston, Virginia, 2010.

[37] PEER. NGA Strong Motion Database. Pacific Earthquake Engineering Research Center, 2010.

[38] Gail, A., Karen, A., Bernie, D. Engineering seismology toolbox; 2009.

[39] Naumoski, N., Saatcioglu, M., and Amiri-Hormozaki, K. Effects of Scaling of earthquake excitations on the dynamic response of reinforced concrete frame buildings. 13th World Conference on Earthquake Engineering, August 1-6, 2004, Vancouver, B.C., Canada.

[40] Goel, R.K., and Chopra, A.K. Period formulas for moment-resisting frame buildings. Journal of Structural Engineering 1997; 123(11): 1454-146.

[41] Moheit, W. Schubbeulung rechteckiger Platten mit eingespannten Rändern. Thesis, Technische Hochschule Darmstadt, Leipzig, Germany; 1939.

[42] Choi, B. J., Kim, K. Y., Kim, C. H., and Kim, T. Y. Experimental Compression Behavior of Stiffened Steel Plate Concrete (SSC) Structures under Compression Loading. Proceedings of 20th International Conference on Structural Mechanics in Reactor Technology (SMiRT 20), Division 5; 2009; Espoo, Finland, August 9-14.

[43] Timoshenko, S.P., and Gere, J. M. Theory of Elastic Stability. McGraw-Hill: New York; 1961.

Figure Captions for "Seismic performance of composite plate shear walls"

Sandip Dey and Anjan K. Bhowmick
Department of Building, Civil and Environmental Engineering, Concordia University, Montreal, Quebec, Canada

Fig. 1. Concrete damage plasticity model: (a) Concrete tension stiffening curve; (b) Concrete tension damage curve
Fig. 2. Concrete damage plasticity model: (a) Concrete compression hardening curve; (b) Concrete compression damage curve
Fig. 3. Validation of Zhao and Astaneh-Asl (2004) innovative specimen: (a) FE mesh; (b) Push-over curves
Fig. 4. Validation of cyclic curves for Zhao and Astaneh-Asl (2004) innovative specimen

Fig. 5. Validation of cyclic curves for Driver et al. (1998) SPSW test

Fig. 6. Load deformation relations of C-PSW tests by Zhao and Astaneh-Asl (2004)

Fig. 7. Floor plans of sample buildings: (a) For C-PSWs with aspect ratio 1.0; (b) For C-PSWs with aspect ratio 1.5

Fig. 8. 4-storey and 6-storey C-PSWs (aspect ratio 1.0)

Fig. 9. Analytical model for 4-storey C-PSW

Fig. 10. Acceleration spectra for selected accelerograms and design spectra for Vancouver:
(a) for 4-storey C-PSW; (b) for 6-storey C-PSW
Fig. 11. Average peak storey shear contributions of 4-storey and 6-storey C-PSWs

Fig. 12. Peak column axial force and moment of 4- storey C-PSW

Fig. 13. Peak column axial force and moment of 6-storey C-PSW

Fig. 14. FE mesh of 6-storey (left) and 4-storey (right) C-PSW (only the critical portion) at peak base shear instant under 7c2 ground motion

Fig. 15. Interstorey drift ratio for 4-storey C-PSW: (a) Under simulated records, (b) Under real earthquake records

Fig. 16. Interstorey drift ratio for 6-storey C-PSW: (a) Under simulated records, (b) Under real earthquake records

Fig. 17. Regression analysis for periods of C-PSWs

Fig. 18. Representation of horizontal and vertical stiffeners in C-PSW

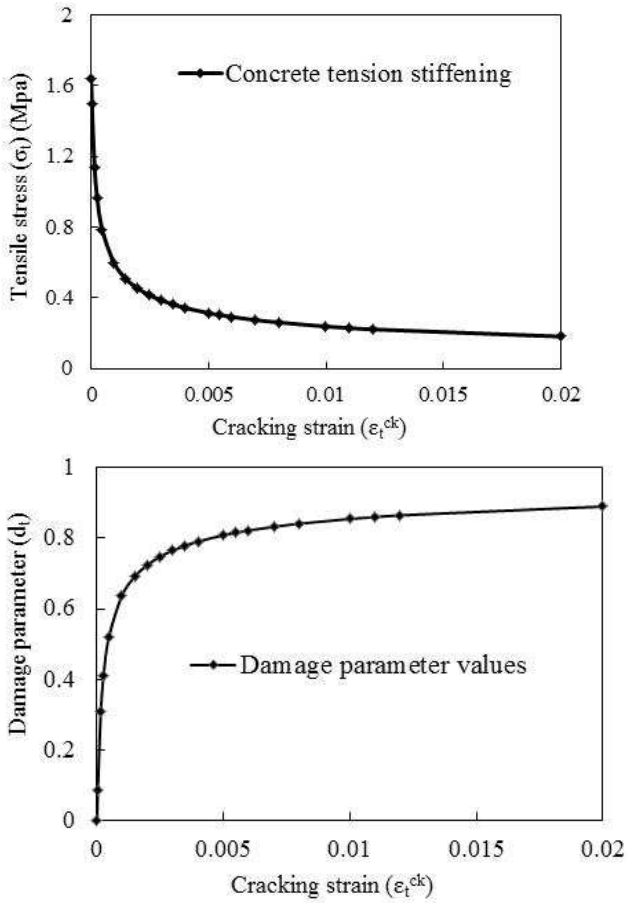

(a) Concrete tension stiffening curve (b) Concrete tension damage curve

Fig. 1. Concrete damage plasticity model: (a) Concrete tension stiffening curve; (b) Concrete tension damage curve

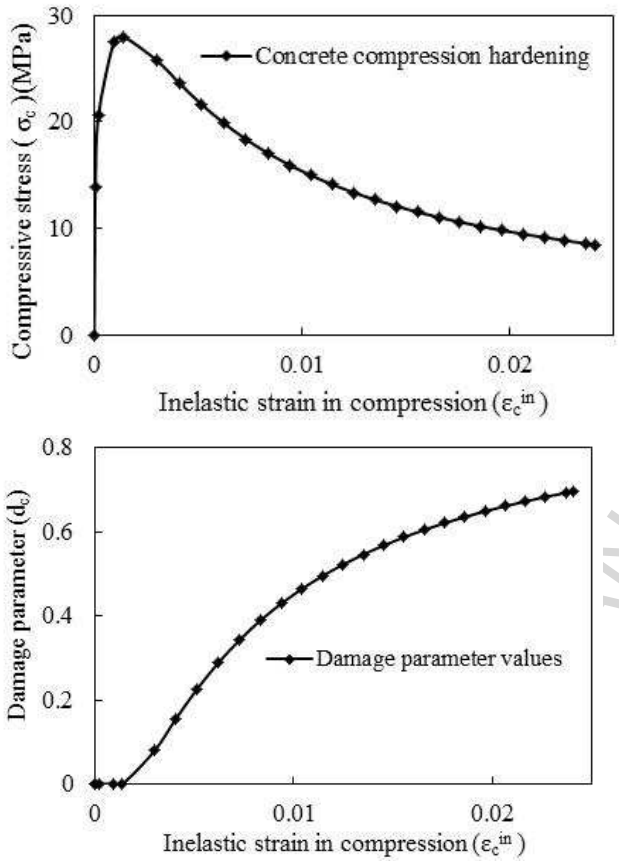

(a) Concrete compression hardening curve (b) Concrete compression damage curve

Fig. 2. Concrete damage plasticity model: (a) Concrete compression hardening curve; (b) Concrete compression damage curve

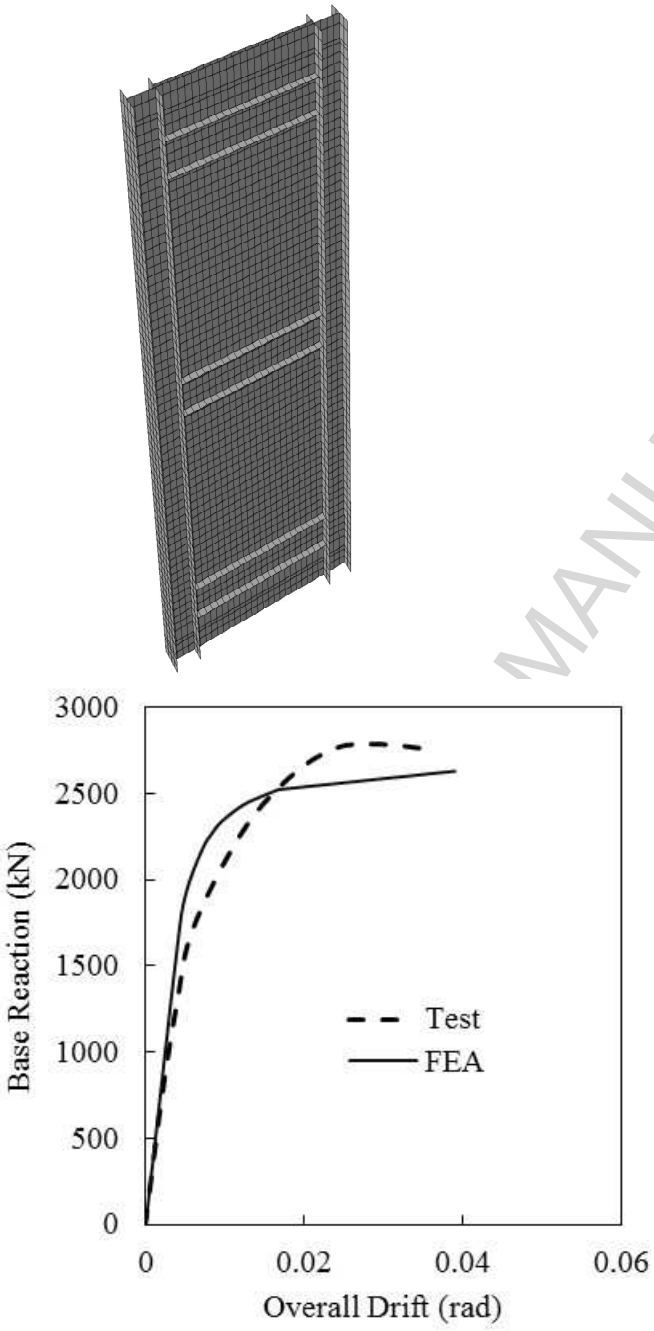

(a) FE Mesh (b) Push-over curves

Fig. 3. Validation of Zhao and Astaneh-Asl (2004) innovative specimen: (a) FE mesh; (b) Push-over curves

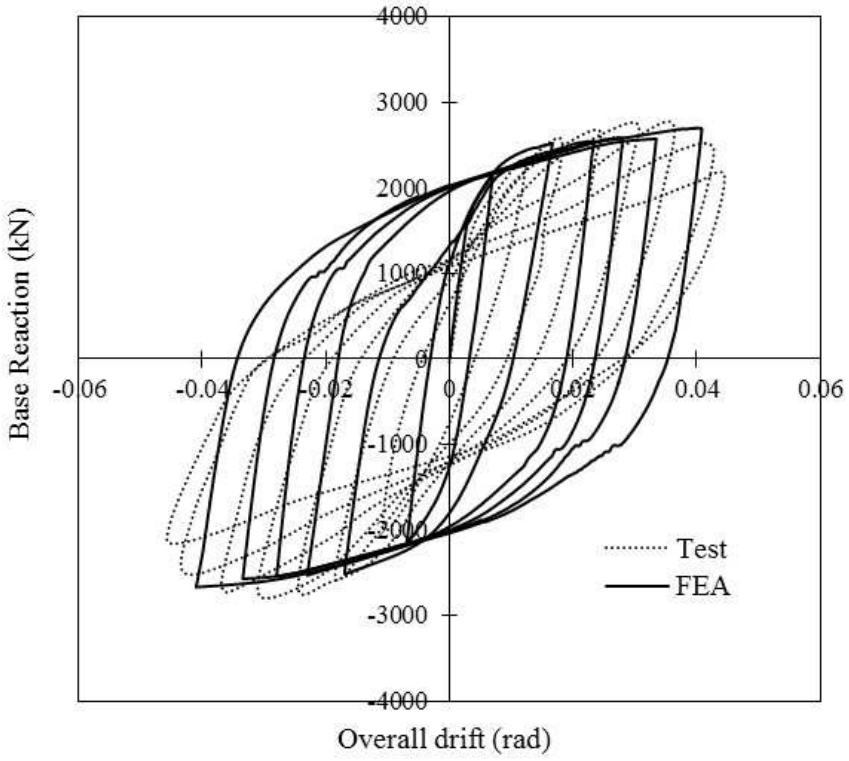

Fig. 4. Validation of cyclic curves for Zhao and Astaneh-Asl (2004) innovative specimen

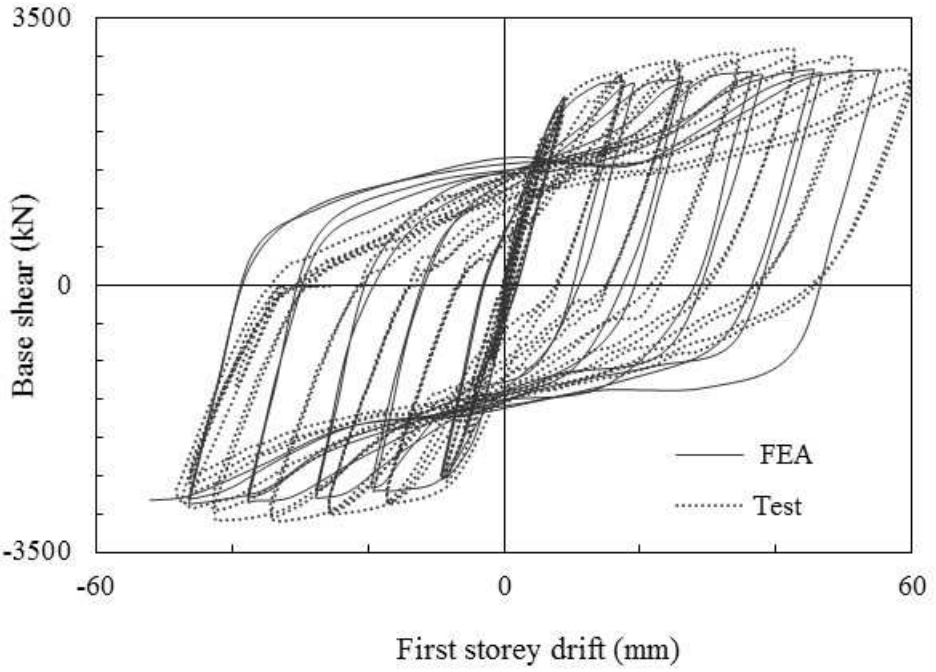

Fig. 5. Validation of cyclic curves for Driver et al. (1998) SPSW test

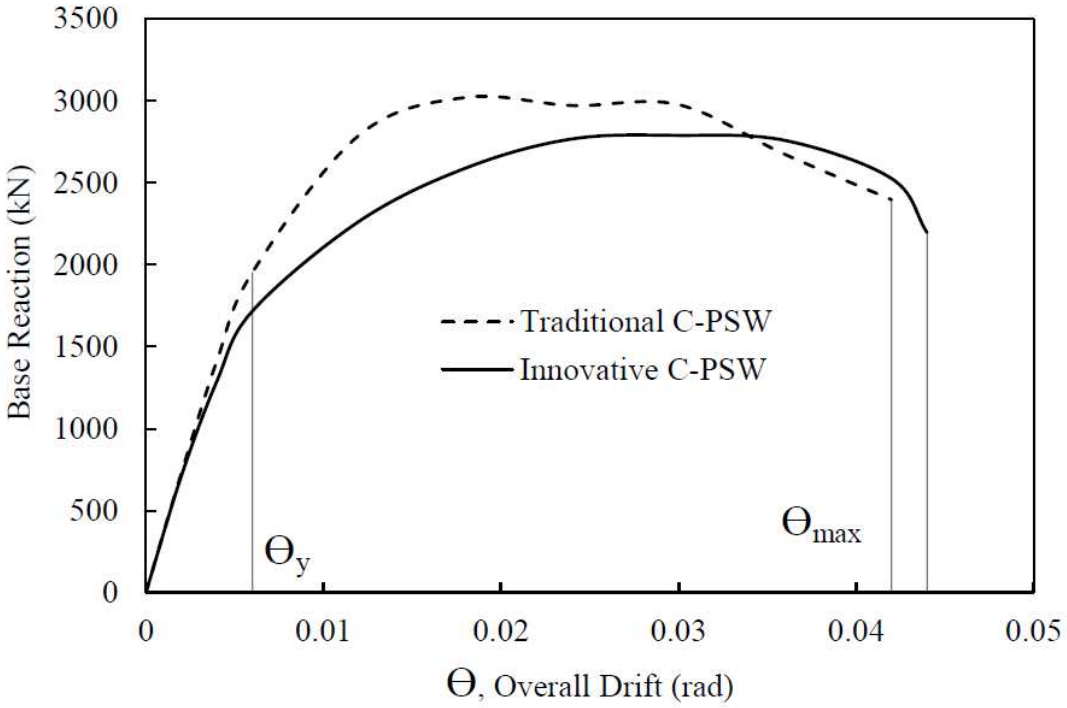

Fig. 6. Load deformation relations of C-PSW tests by Zhao and Astaneh-Asl (2004)

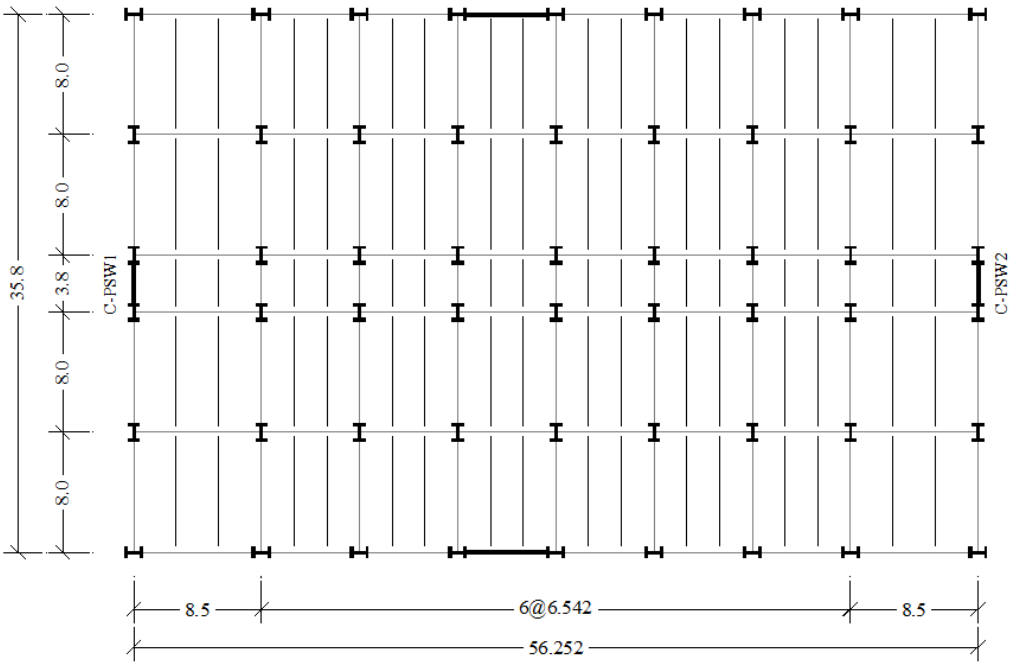

(a) For C-PSWs with aspect ratio 1.0

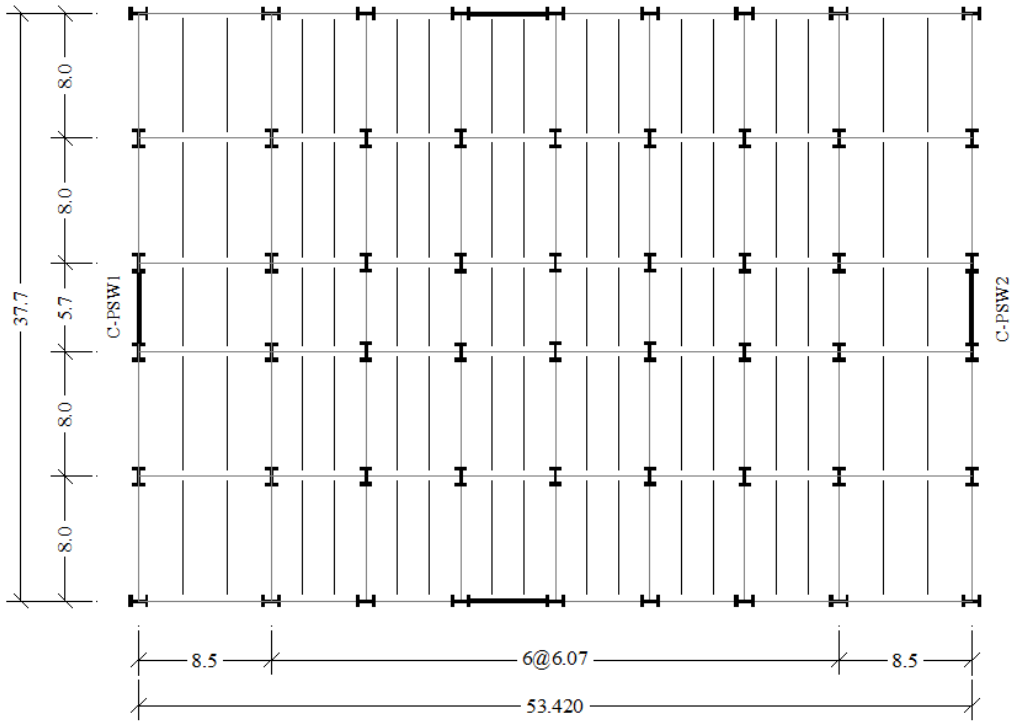

(b) For C-PSWs with aspect ratio 1.5

Fig. 7. Floor plans of sample buildings: (a) For C-PSWs with aspect ratio 1.0; (b) For C-PSWs with aspect ratio 1.5

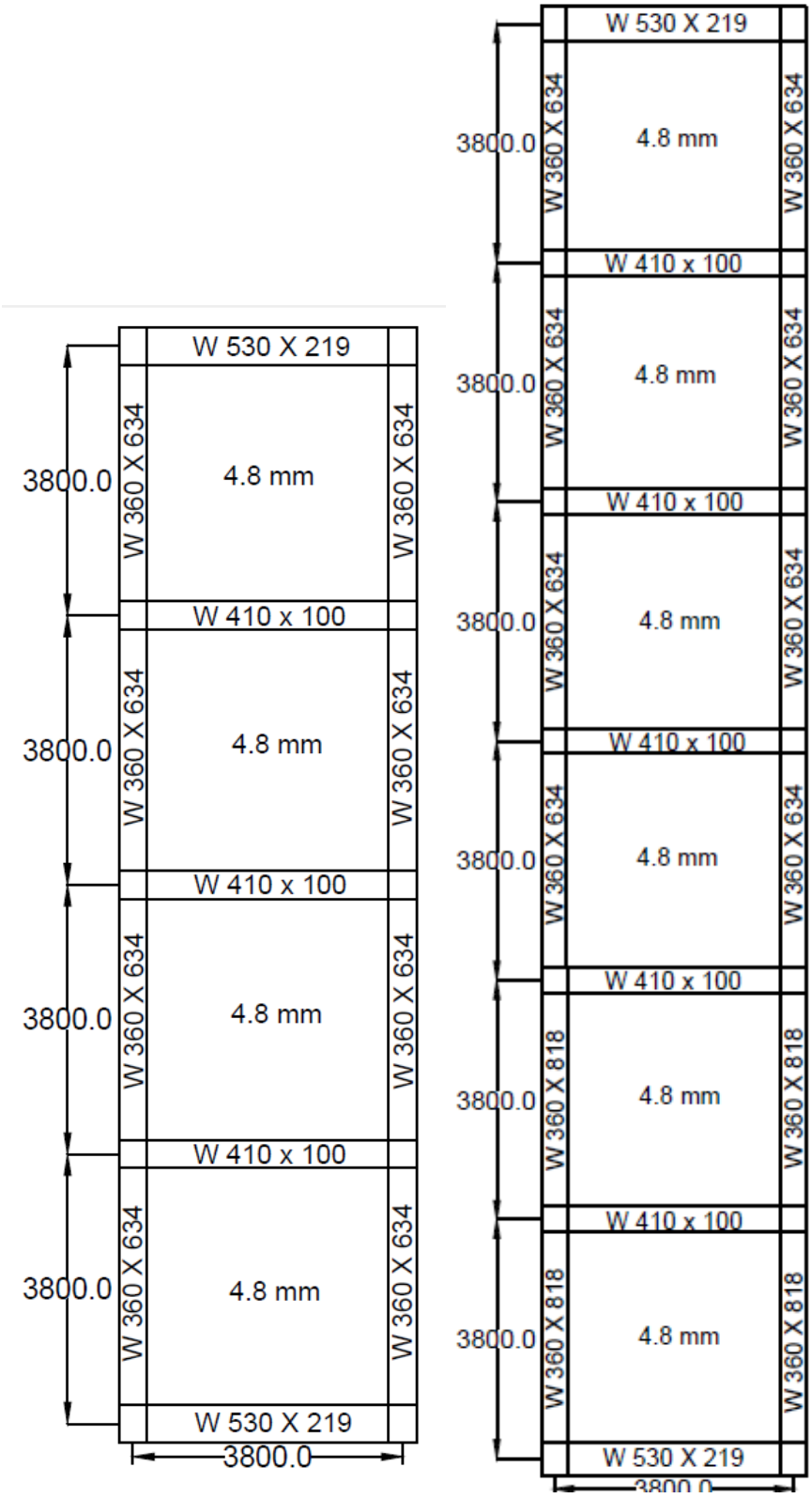

Fig. 8. 4-storey and 6-storey C-PSWs (aspect ratio 1.0)

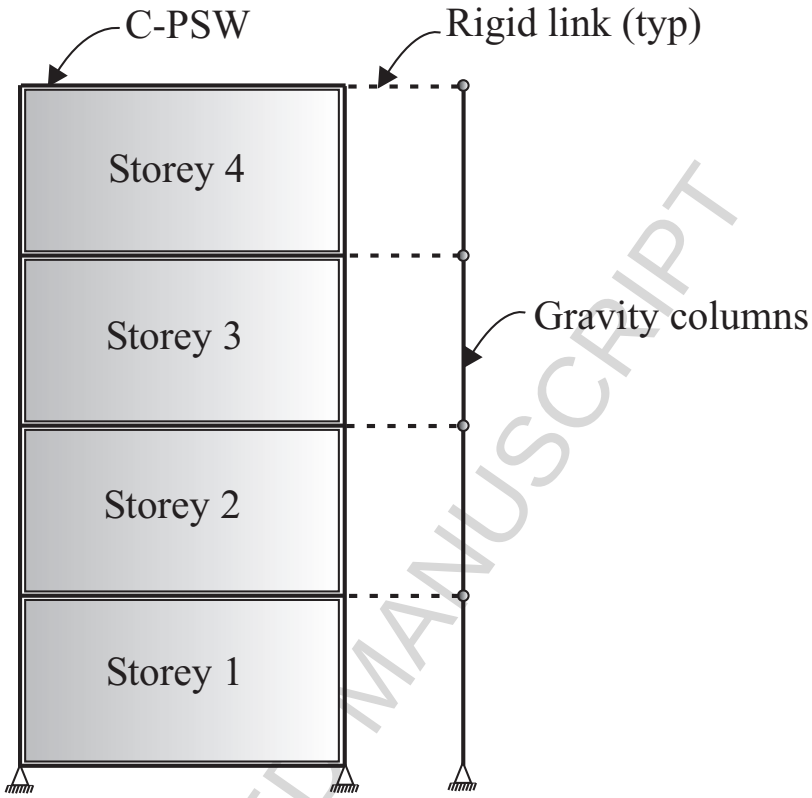

Fig. 9. Analytical model for 4-storey C-PSW

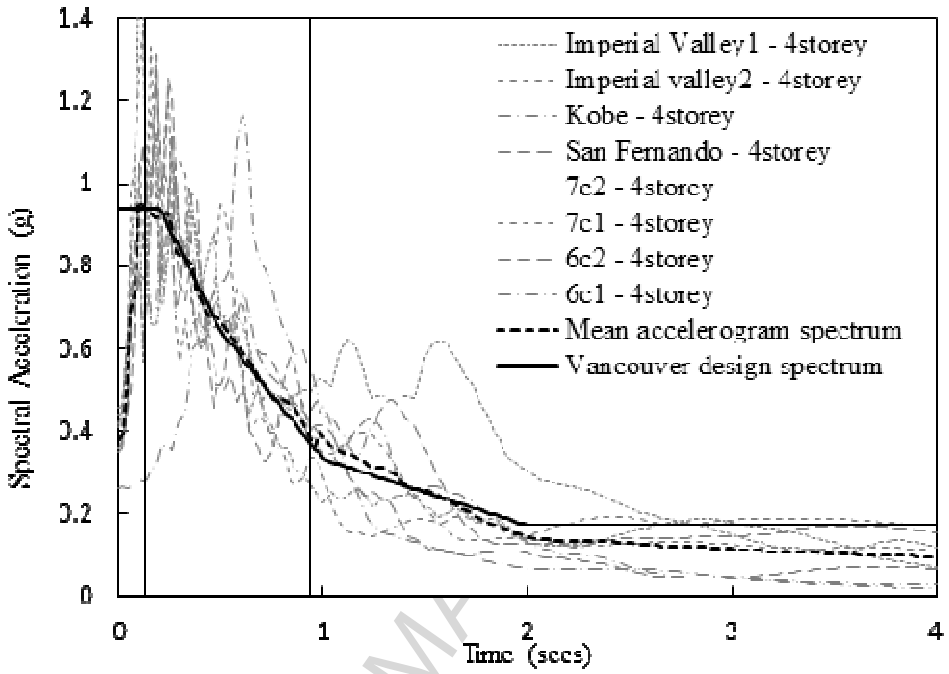

(a) for 4-storey C-PSW

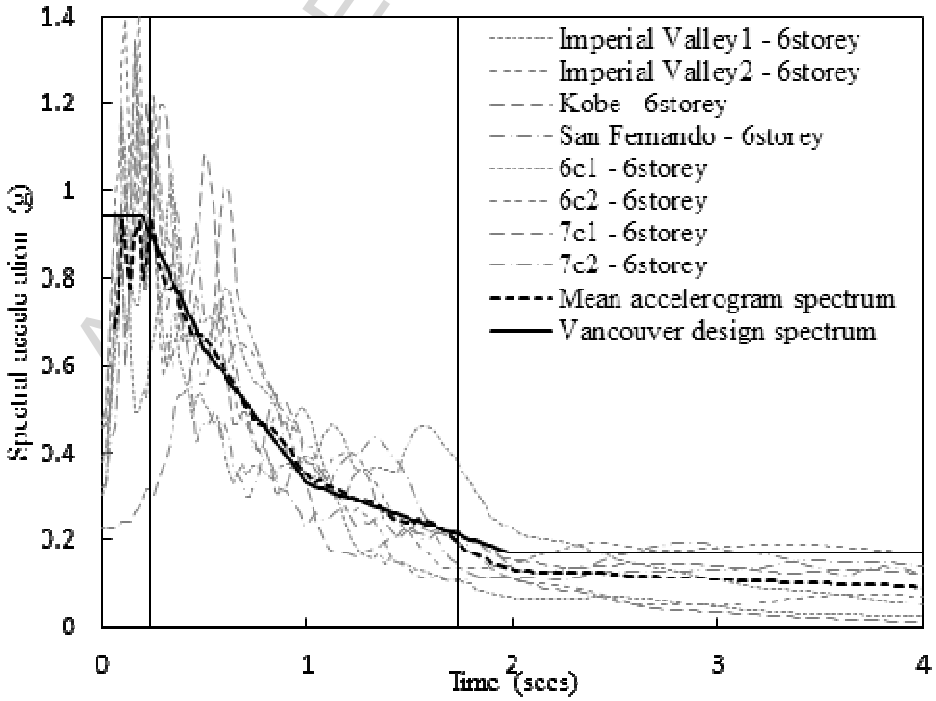

(b) for 6-storey C-PSW

Fig. 10. Acceleration spectra for selected accelerograms and design spectra for Vancouver: (a) for 4-storey C-PSW; (b) for 6-storey C-PSW

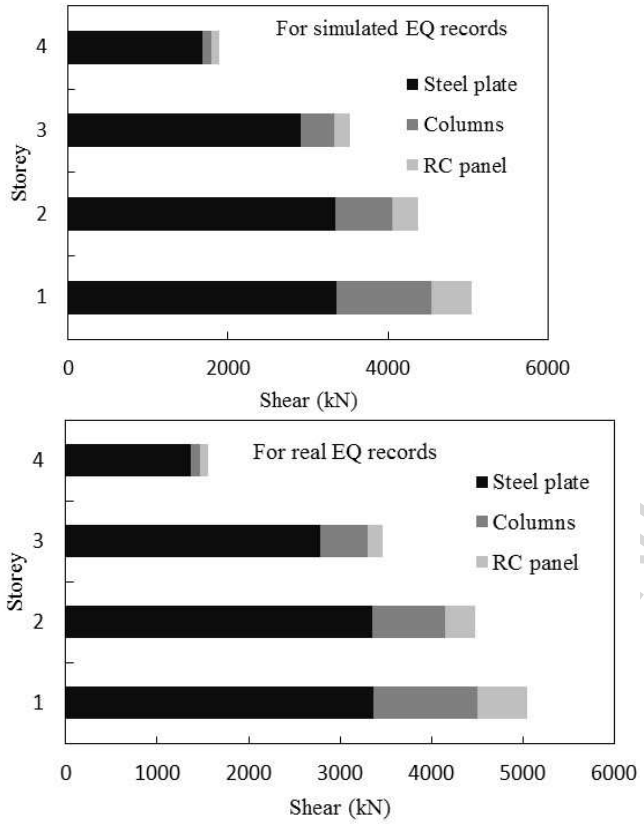

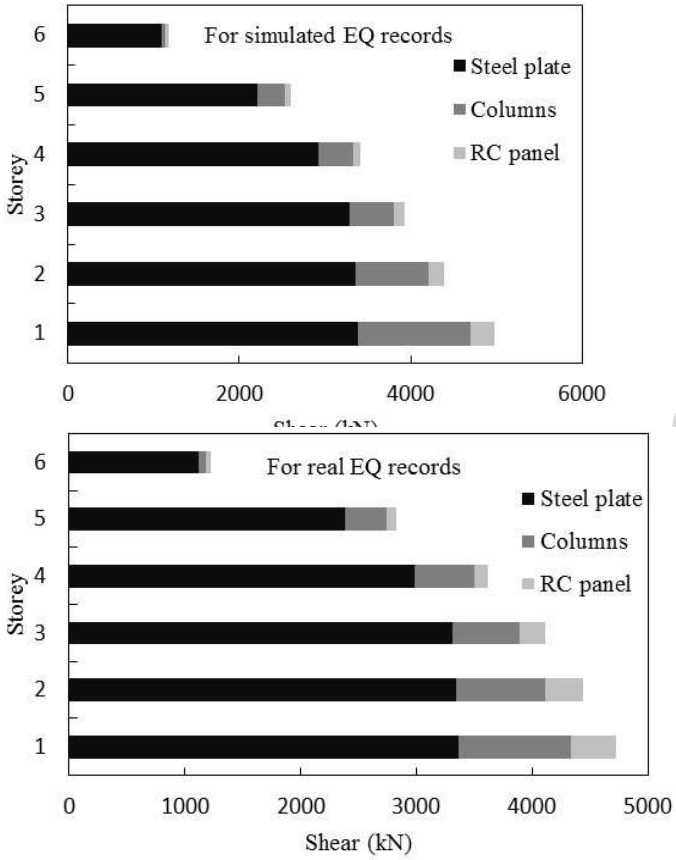

Fig. 11. Average peak storey shear contributions of 4-storey and 6-storey C-PSWs

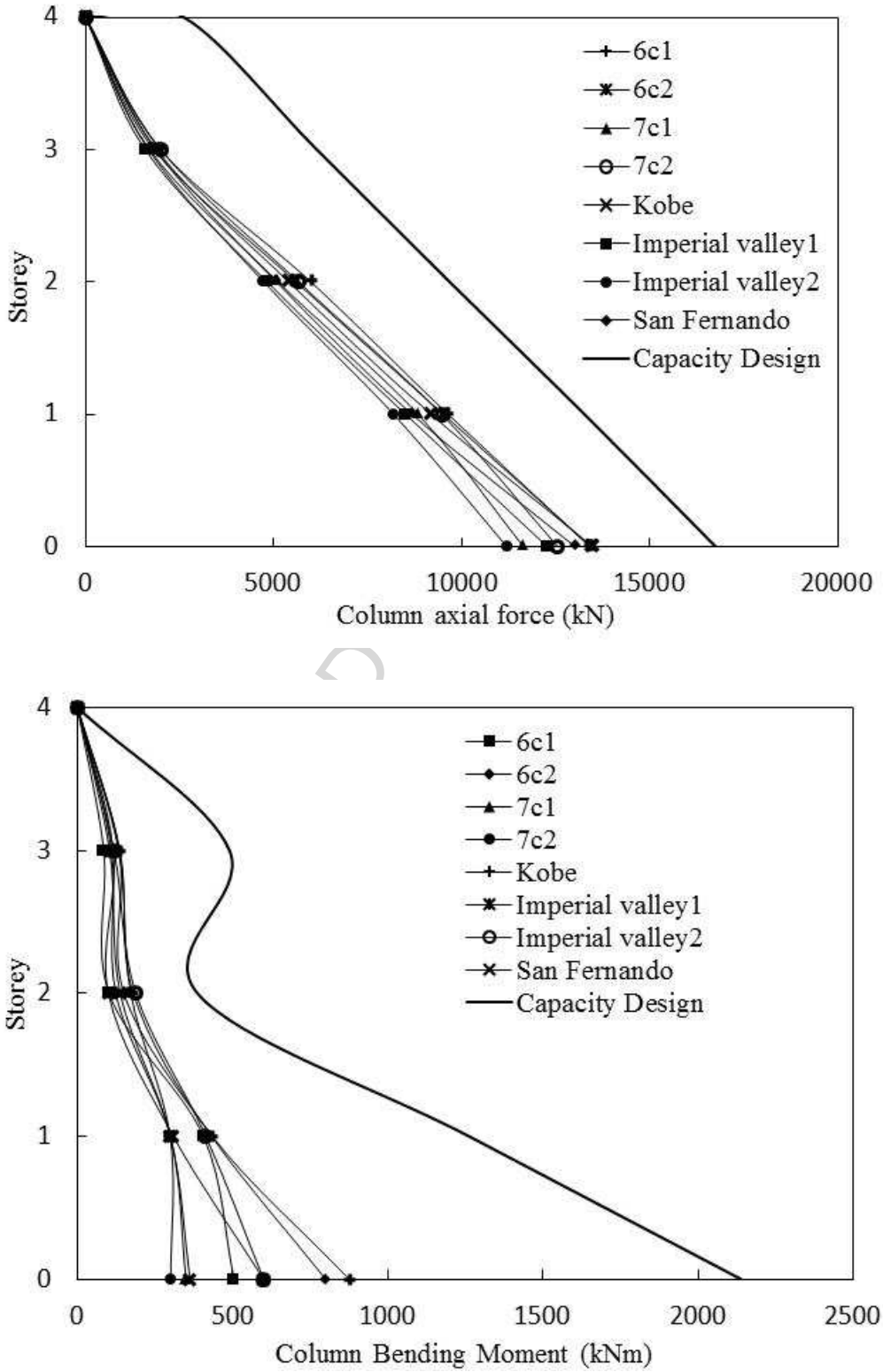

Fig. 12. Peak column axial force and moment of 4- storey C-PSW

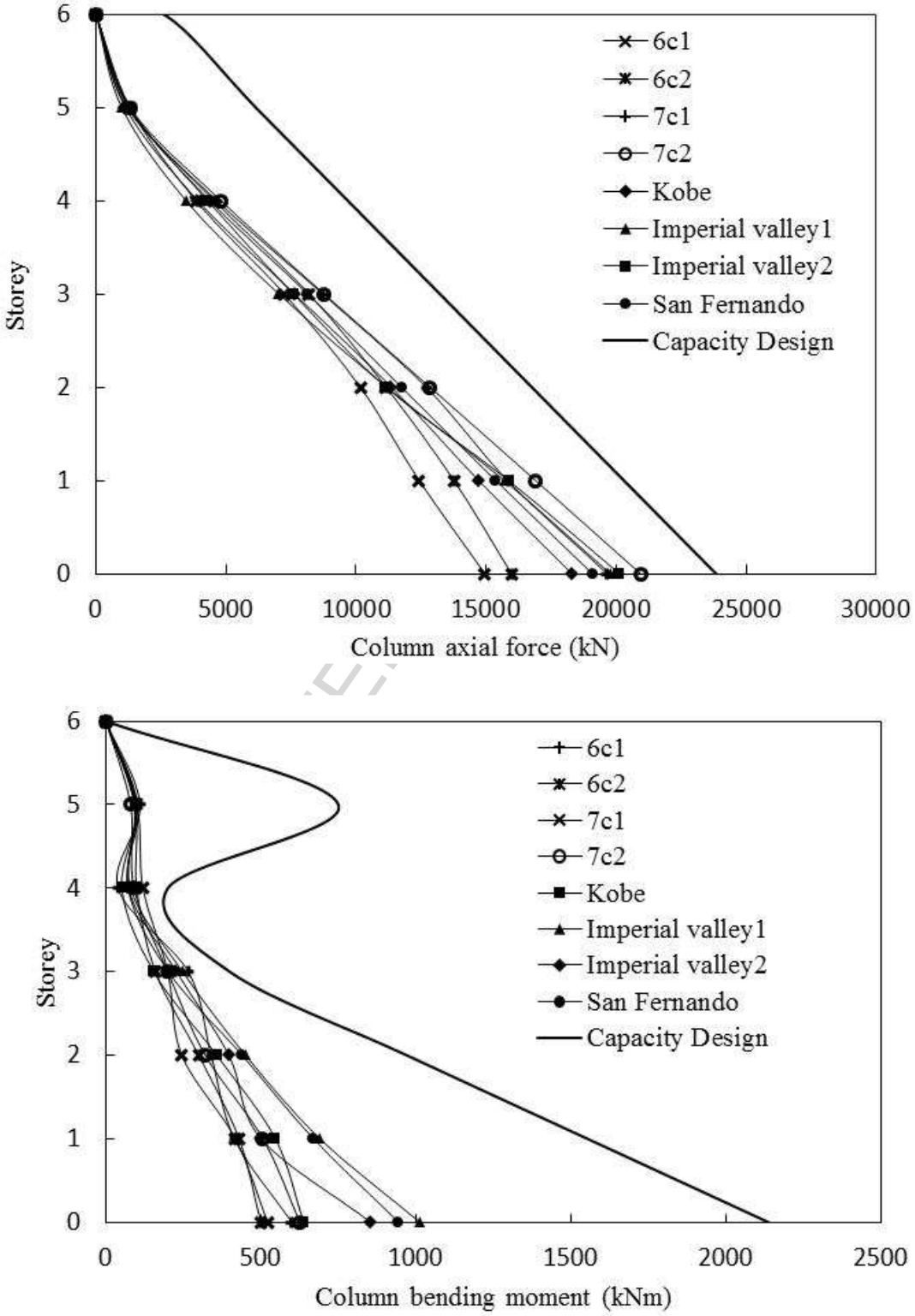

Fig. 13. Peak column axial force and moment of 6-storey C-PSW

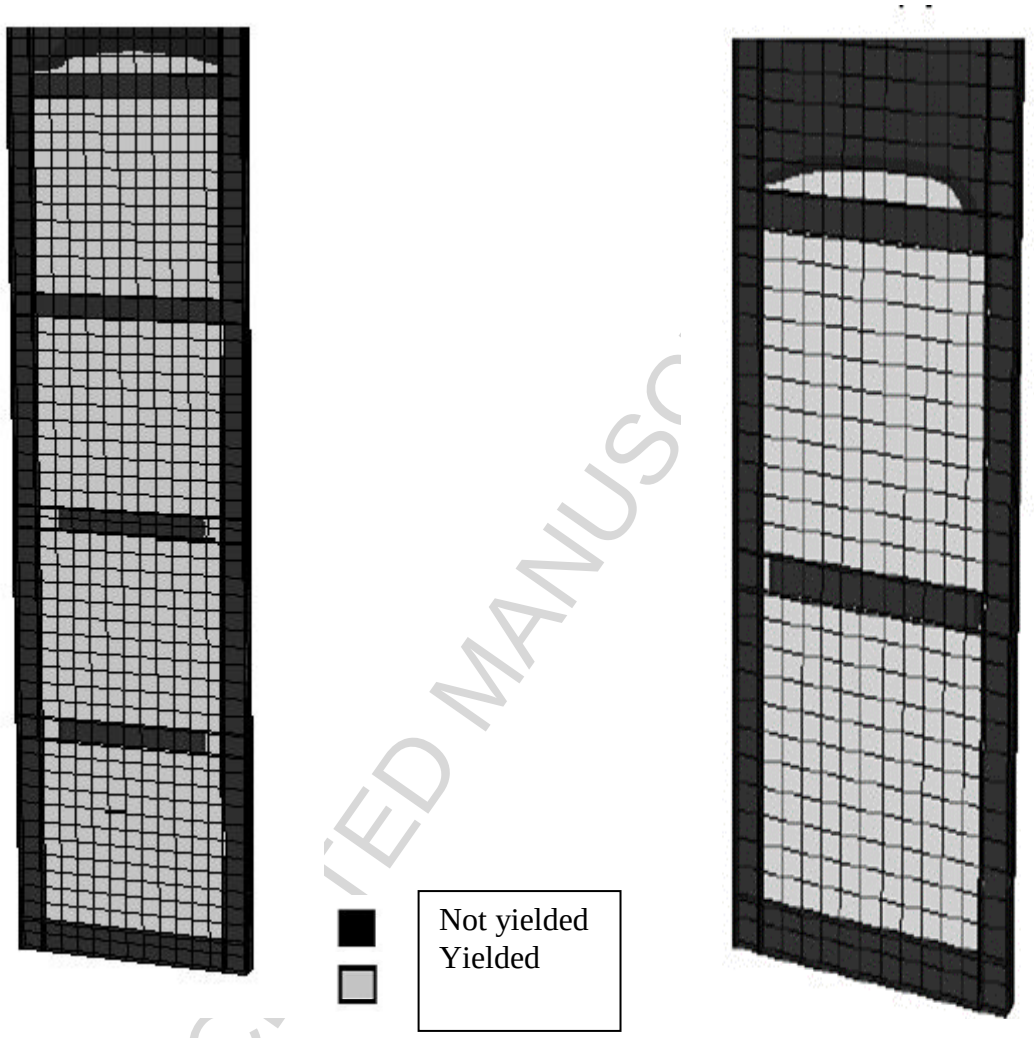

Fig. 14. FE mesh of 6-storey (left) and 4-storey (right) C-PSW (only the critical portion) at peak base shear instant under 7c2 ground motion

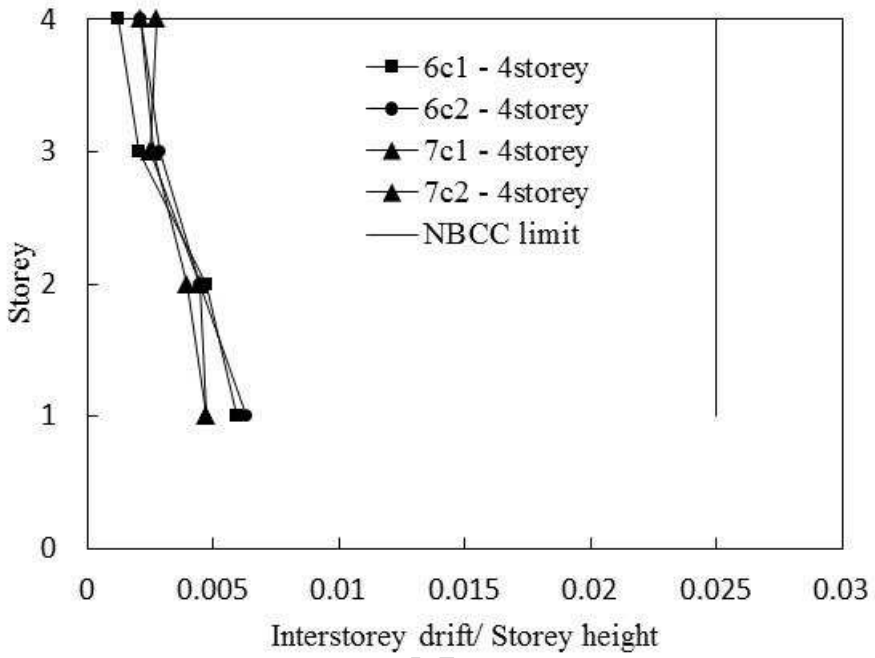

(a) Under simulated records

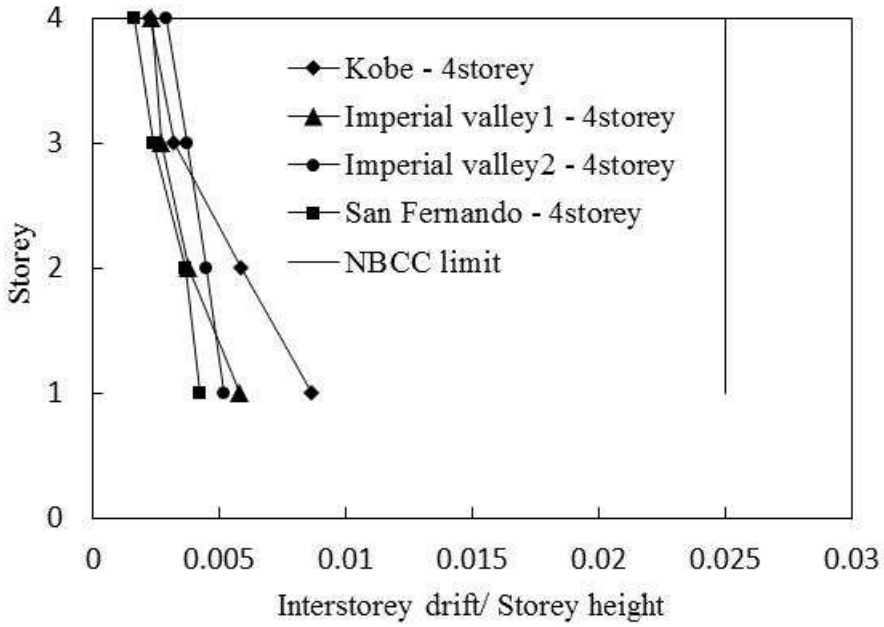

(b) Under real earthquake records

Fig. 15. Interstorey drift ratio for 4-storey C-PSW: (a) Under simulated records, (b) Under real earthquake records

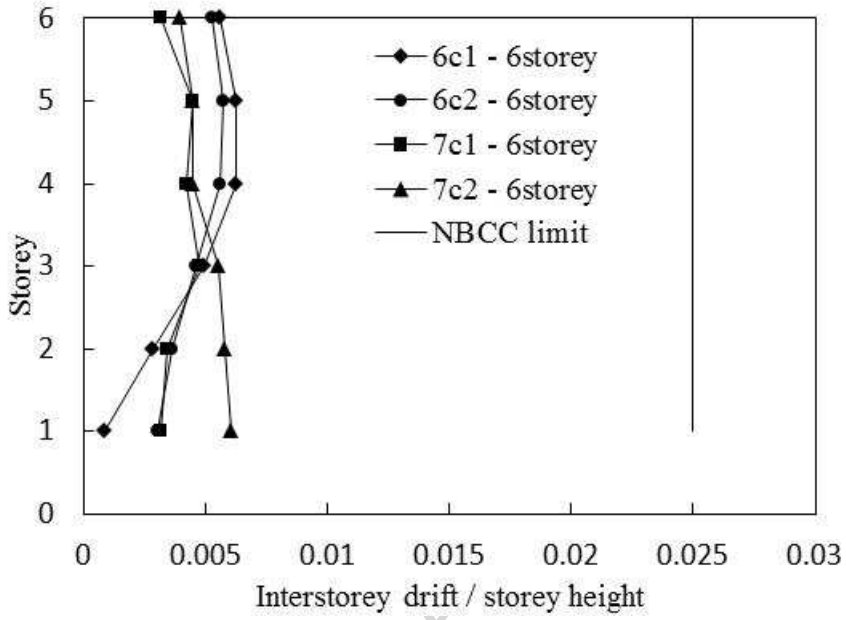

(a) Under simulated records

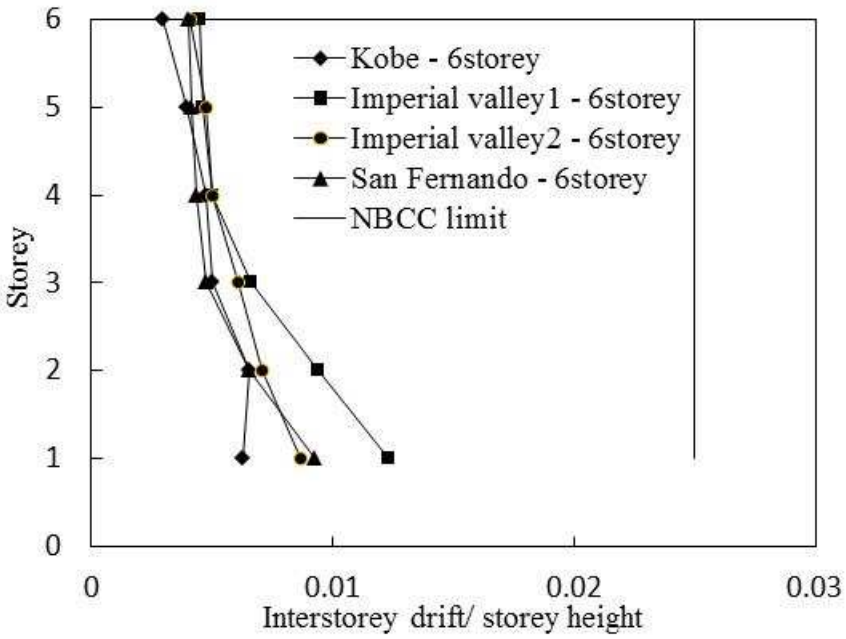

(b) Under real earthquake records

Fig. 16. Interstorey drift ratio for 6-storey C-PSW: (a) Under simulated records, (b) Under real earthquake records

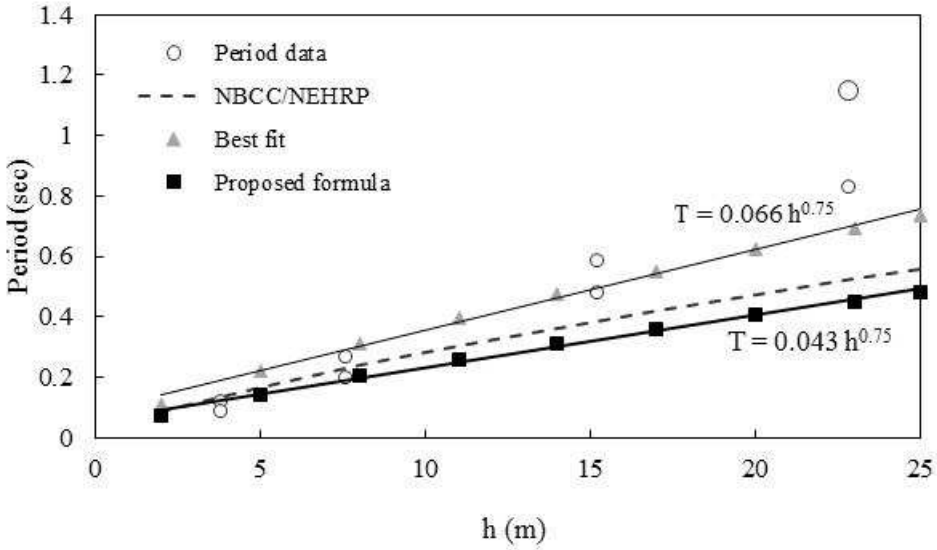

Fig. 17. Regression analysis for periods of C-PSWs

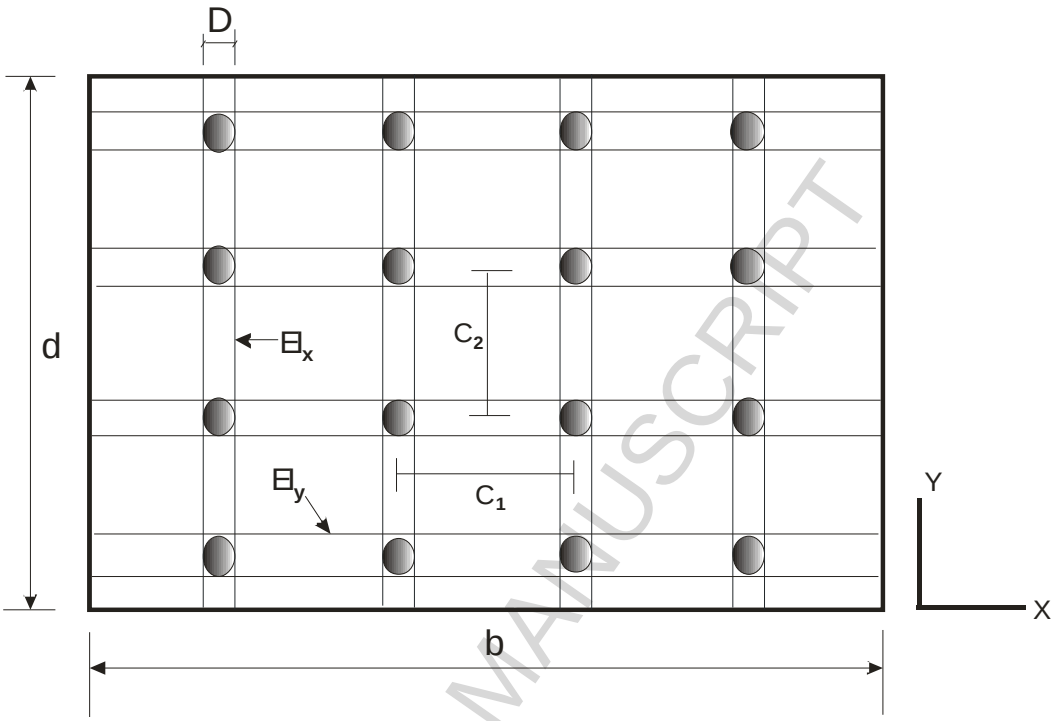

Fig.18. Representation of horizontal and vertical stiffeners in C-PSW

Table 1. Ground motion parameters of selected real ground motions

Event name	Magnitude	Site	Maximum Acceleration A (g)	A/V	Scaling Factors	
					4-storey	6-storey
Kobe, Japan,1995	6.6	HIK	0.143	0.968	1.84	1.60
San Fernando, California, 1971	6.61	La-Hollywood Stor. LOT	0.188	1.04	1.65	1.53
Imperial Valley, California, 1979	6.53	Aeropuerto Maxicali	0.3118	1.03	1.25	0.93
Imperial Valley, California, 1979	6.53	El-Centro array	0.525	1.04	0.99	1.0

Table 2. Parameters of selected simulated earthquake records

Earthquake event name	Magnitude	Maximum Acceleration A (g)	Maximum velocity V (m/s)	A/V	Scaling Factors	
					4-storey	6-storey
6C1	6.5	0.345	0.26	1.33	0.71	0.76
6C2	6.5	0.35	0.266	1.32	1.31	1.44
7C1	7.5	0.426	0.406	1.05	0.79	0.89
7C2	7.5	0.409	0.445	0.92	1.72	1.81

Table 3. Selected C-PSWs for period calculations

C-PSW type	Storey	Aspect ratio 1.0		Aspect ratio 1.5	
		Column sections	Top/base beam section	Column sections	Top/base beam section
1-storey	1	W360×421	W530×219	W360×744	W610×372
2-storey	1-2	W360×509	W530×219	W360×744	W610×372
4-storey	1-4	W360×634	W530×219	W360×818	W610×372
6-storey	1-2	W360×818	W530×219	W360×990	W610×372
	3-6	W360×634	W530×219	W360×677	W610×372

Steel plate thickness = 4.8 mm, Concrete panel thickness = 200 mm
All intermediate beams are W410x100 for Aspect ratio 1.0
All intermediate beams are W410x132 for Aspect ratio 1.5